



CHALMERS
UNIVERSITY OF TECHNOLOGY



Investigation of ship ice-resistance in the marginal ice zone

Master's thesis in the International Master's Program of Naval Architecture and Ocean Engineering

HUIXUAN XIAO

Department of Mechanics and Maritime Sciences
CHALMERS UNIVERSITY OF TECHNOLOGY
Gothenburg, Sweden 2019
Master's Thesis 2019/79

MASTER'S THESIS IN THE INTERNATIONAL MASTER'S PROGRAM IN NAVAL
ARCHITECTURE AND OCEAN ENGINEERING

Investigation of ship ice-resistance in the marginal ice zone

HUIXUAN XIAO

Department of Mechanics and Maritime Sciences

Division of Marine Technology

CHALMERS UNIVERSITY OF TECHNOLOGY

Göteborg, Sweden 2019

Investigation of ship ice-resistance in the marginal ice zone
HUIXUAN XIAO

© HUIXUAN XIAO, 2019

Master's Thesis 2019/79
Department of Mechanics and Maritime Sciences
Division of Marine Technology
Chalmers University of Technology
SE - 412 96 Göteborg
Sweden
Telephone: + 46 (0)31-772 1000

Cover: Ice-going ship picture from News: International team of researchers release status report on changing Arctic

Printed by Chalmers Reproservice
Göteborg, Sweden 2019

Investigation of ship ice-resistance in the marginal ice zone
Master's Thesis in the International Master's Programme in Naval Architecture and Ocean Engineering

HUIXUAN XIAO

Department of Mechanics and Maritime Sciences

Division of Marine Technology

Chalmers University of Technology

Abstract

Under the influence of global warming, the Arctic ice sheet area has been decreasing. As a consequence, vessel traffic has been increasing rapidly in the Arctic. Most Arctic traffic occurs in summer when ice coverage is at its lowest level. Therefore, the impact of brash ice and broken ice on ship resistance is relevant to study during the Arctic summer.

The aim of this thesis was to compare ice resistance prediction models for brash ice conditions and broken ice conditions, respectively. Three groups of experiment data from literatures were compared in a case study. By comparing the model estimates and the experiment results, the applicability of each model was discussed and summarized. The Spencer and Jones model for brash ice and broken ice was found to give rather good performance prediction and was thus applied for calculation of ship performance of Arctic transit ships.

In addition, a sensitivity study was carried out to investigate the impact on the ice resistance from the various parameters of ice and ship hull. It was found that the ice thickness and ice concentration have the greatest influence on the resistance in all the models.

With the selected models, the corresponding fuel consumptions and sailing time for a part of the Northern Sea Route was simulated and compared under different ice conditions. The ice was real-life records of July, October, and November in 2018. The results indicated that severe ice conditions and a higher speed lead to significant increases of fuel consumption.

Keywords: brash ice, broken ice, ice resistance, marginal ice zone, semi-empirical models.

Table of contents

Abstract.....	I
Table of contents	III
Preface.....	V
Nomenclature	VII
1 Introduction.....	1
1.1 <i>Background and Motivation of Study</i>	<i>1</i>
1.2 <i>Objectives and goals</i>	<i>3</i>
1.3 <i>Delimitations.....</i>	<i>3</i>
1.4 <i>Outline of methodology.....</i>	<i>3</i>
2 Sea ice characteristics	5
2.1 <i>Difference sea ice types</i>	<i>5</i>
2.2 <i>Physical properties of sea ice</i>	<i>7</i>
2.2.1 <i>Ice thickness.....</i>	<i>7</i>
2.2.2 <i>Ice salinity and porosity</i>	<i>8</i>
2.2.3 <i>Ice density and temperature</i>	<i>8</i>
2.2.4 <i>Friction angle</i>	<i>9</i>
2.3 <i>Previous ice models</i>	<i>10</i>
3 Ice resistance models.....	11
3.1 <i>Broken ice</i>	<i>11</i>
3.1.1 <i>The Guo model</i>	<i>11</i>
3.1.2 <i>The Woolgar and Colbourne model.....</i>	<i>12</i>
3.2 <i>Brash ice</i>	<i>13</i>
3.2.1 <i>The Spencer and Jones model.....</i>	<i>13</i>
3.2.2 <i>The Riska model</i>	<i>14</i>
3.2.3 <i>The Mellor model</i>	<i>16</i>
3.3 <i>Model summary.....</i>	<i>17</i>
4 Description of case study	19
4.1 <i>Input values.....</i>	<i>19</i>
4.2 <i>Comparison for Case 1</i>	<i>19</i>
4.3 <i>Comparison for Case 2</i>	<i>21</i>
4.4 <i>Comparison for Case 3</i>	<i>23</i>
4.5 <i>Summary of case study.....</i>	<i>25</i>

5	Results and discussion	27
5.1	<i>Sensitivity analysis</i>	27
5.1.1	Ice density	27
5.1.2	Ice thickness.....	29
5.1.3	Ice concentration.....	30
5.1.4	Ice-hull friction coefficient	31
5.1.5	Results and discussion of sensitivity study	32
5.2	<i>Ice resistance module of the ShipCLEAN model</i>	32
5.3	<i>Ship route</i>	33
6	Summary and conclusions.....	39
7	Future work.....	41
8	References.....	43
	Appendix A: Results of case study	47
	Appendix B: Results of sensitivity analysis	49
	Appendix C: ShipCLEAN results of propulsion power and fuel consumption rate	53

Preface

This thesis is a part of the requirements for the master programme of Naval Architecture and Ocean Engineering at the Department of Mechanics and Maritime Sciences at Chalmers University of Technology.

I would like to acknowledge and thank my examiner and supervisor, Professor Jonas Ringsberg at the Department of Mechanics and Maritime Sciences for the time and supervision he has given me. I would also like to thank my co-supervisor Zhiyuan Li for all help and support throughout this thesis.

Gothenburg, June 2019

Huixuan Xiao

Nomenclature

List of acronyms

EG/AD/S	Ethylene Glycol, Aliphatic Detergent and Sugar
FPSO	Floating Production Storage and Offloading
HSVA	Hamburg Ship Model Basin
IMD	Institute for Marine Dynamics (now is known as National Research Council's Institute for Ocean Technology, Canada)
ISO	International Standard Organization
ITO	Institute for Ocean Technology
KCS	Kriso Container Ship
MIZ	Marginal Ice Zone
POAC	The Port and Ocean Engineering under Arctic Conditions
UN SDGs	United Nations Sustainable Development Goals

List of unit abbreviations

deg	degrees
kg	kilograms
kn	knots
kW	kilowatt
m	meters
N	newtons
Pa	pascal
ppt	parts-per-trillion
s	seconds
t	tonne

Variables

<i>Sea ice properties</i>		<i>Unit</i>
μ_B	$(1 - p)$ (p is ice porosity, $\mu_B = 0.8 - 0.9$)	-
ρ_i	ice density	kg/m ³
σ_1	the maximum principle stress in the shearing plane	Pa

σ_3	the minimum principle stress in the shearing plane	Pa
\emptyset	angle of shear resistance (also called friction angle)	deg
C	concentration, the percentage of sea surface covered by ice	-
h_F	the thickness of brash ice layer on the side	m
h_i	ice thickness	m
h_M	the thickness of the brash ice in the middle of the channel	m
K_0	lateral stress coefficient at rest	-
K_p	passive stress coefficient	-
S_i	ice salinity, a ratio of salt weight in grams per kilogram of sea water	ppt or ‰
t	freezing time	day
T	ice temperature	°C
T_a	temperatures at the top of the ice or the ambient air temperature	°C
T_b	temperatures at the bottom of the ice	°C
v_a	relative gas or air volume in the ice	-
v_b	relative brine in the ice	-
v_t / n	total ice porosity	-

<i>Ship parameters</i>		<i>Unit</i>
μ_e	effective friction coefficient	-

β	the angle between the waterline and the vertical at $B/2$	deg
A_{WF}	foreship waterline area	m ²
B	ship beam	m
f	ship-ice friction coefficient	-
Fn	Froude number	-
L	ship length	m
L_{par}	parallel body length	m
T	ship draught	m
α	waterline entrance angle	deg
β''	the apex half-angle of the wedge shape bow	deg
λ	scale factor	-

<i>Parameters in resistance</i>		<i>Unit</i>
C_{ow}	open-water resistance coefficient	-
Fp	pack ice Froude number	-
C_p	pack ice resistance coefficient	-
B	ship beam	m
g	gravity constant	m/s ²

1 Introduction

This chapter introduces the background of sea ice resistance study and the motivation of the thesis study. Objectives and goals are set for this thesis and due to the time limit some delimitations are illustrated first.

1.1 Background and Motivation of Study

Sea ice is a complex material formed by the freezing of sea water. Sea ice covers about 7% of the Earth's surface and about 12% of the world's oceans (Weeks & Hibler, 2010). With the development and utilization of the ocean, the interaction of sea ice with structures such as ships or platforms has a crucial impact on equipment safety and reliability. However, the physical and mechanical properties of sea ice are not static. They are dependent on ice freezing time, temperature, salinity, and other factors. In addition, ice thickness and ice density are also importance factors during ice-structure interaction prediction. The description of sea ice distribution in the following part is based on the review of Weeks and Hibler (2010). Approximate values for the surface areas of the Earth's sea ice distributions can be found in table 1.1.

Table 1.1: Approximate values for the surface areas of the Earth's sea ice distributions. These values can be taken as reasonable estimates for the time period 1950 to ~1980. (Weeks & Hibler, 2010).

Sea ice areas		($\times 10^6 \text{km}^2$)
Northern Hemisphere	Maximum extent	~ 15
	Minimum extent	~ 8
Southern Hemisphere	Maximum extent	~ 18
	Maximum extent	~ 3

Sea ice in the northern hemisphere does not advance parallel to the latitude line. In the Atlantic and Pacific regions, the westward advancement of these ocean basins far exceeds the eastward propulsion. In addition, the presence of shallow water is greatly beneficial to the occurrence of sea ice. In the summer, ice mainly retreats into the Arctic Basin, as well as the northern islands of the Canadian Arctic Islands and the southern part of the east coast of Greenland, known as the East Greenland Drift Stream.

In the southern hemisphere, sea ice is reduced to nearly one sixth of the maximum area at the end of the summer. At the maximum extent, ice is farthest from the continent in the South Atlantic and South Pacific, while ice in the Indian Ocean has the least progress. At the greatest extent, sea ice occurs in a quite thin belt around the continent. However, there are also several so-called ice massifs, even in the late summer, heavy sea ice can still be found in southern hemisphere. In addition, between the maximum and minimum seasonal ice limits, there is a rather wide space, which is significant for all kinds of activities in the ocean, called marginal ice zone (MIZ). MIZ is that part of the ice-covered sea which is close enough to the open ocean boundary to be affected by its presence (Wadhams, 1986). As ice floes are distributed sparsely in MIZ, Eguíluz, et al. (2016) found that higher shipping activity was found to occupy 57-80% of ice-free water in the Arctic area. Especially during summertime, ice coverage is at its lowest level, allowing vessels to be most active.

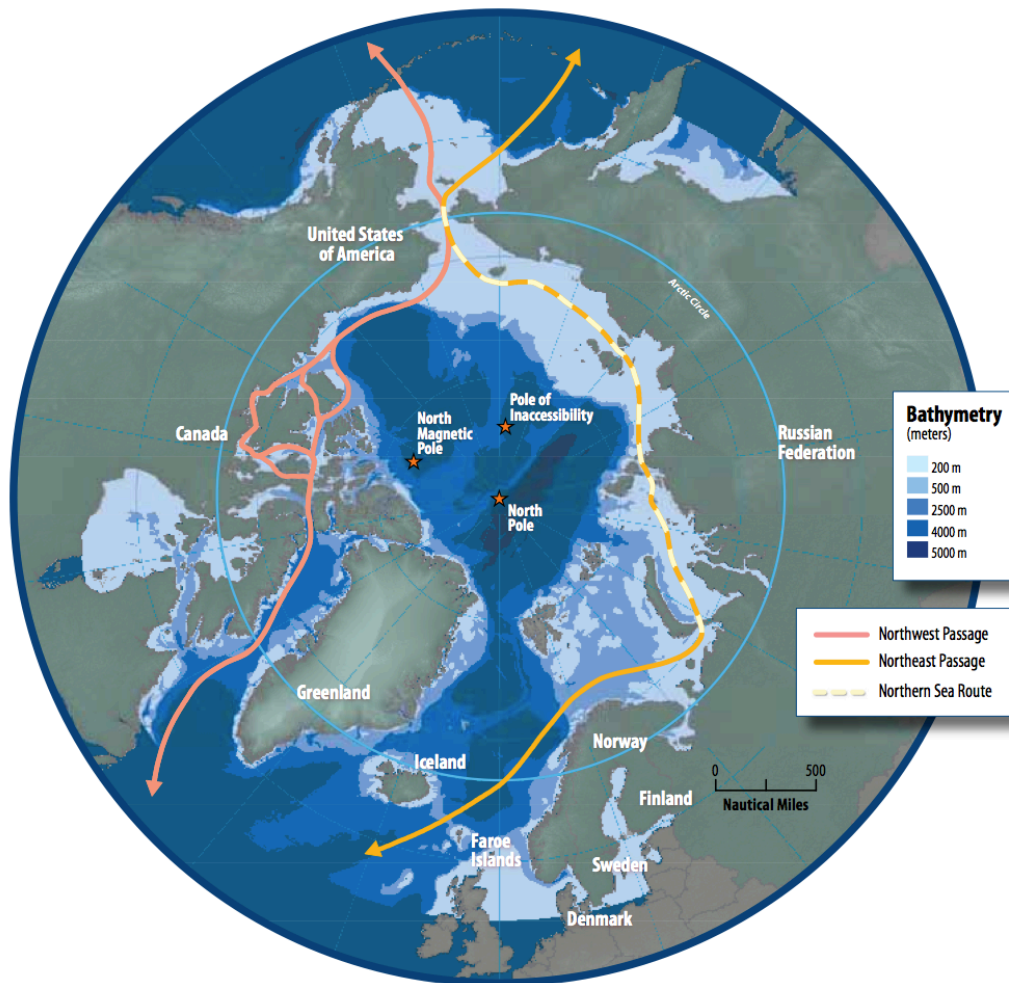


Figure 1.1: Map of the Arctic region showing shipping routes Northeast Passage, Northern Sea Route, and Northwest Passage, and bathymetry (Harder, 2009).

Figure 1.1 shows the existing Arctic routes, which are the shortest routes connecting the three economic zones of Europe, Asia and North America and have very important commercial significance and strategic position (Weeks & Hibler, 2010). Also, abundant oil and mineral resources in the Arctic area need to be explored and transported through these routes (Eguíluz, et al., 2016). Route development within this ice-ocean boundary area can achieve a balance between shortening the sailing time and acceptable required power for ice-going ships to save costs and time, compared with the traditional route through the Suez canal (Wan, et al., 2018). At the same time, it could help to reduce fuel consumption and produce less emissions during the transportation and contribute to UN SDGs (United Nations Sustainable Development Goals) 7,13 and 14. At the same time, under the influence of global warming, the area of Arctic ice sheet has been decreasing year by year and the Arctic sea surface is less covered by ice especially at summer time, which makes it more feasible for regular ships to run in the Arctic area, if those ships have enough safety margins against local failure and power for additional ice resistance. Besides, all the existing routes shown in figure 1.1 are within the Arctic MIZ. Hence, MIZ as a partly ice-covered area is the most possible area for the conventional vessels to run through without the assistance of icebreakers. In this case, it is of vital importance to analyse ship ice-resistance in MIZ for naval architects to ensure both ice-going ship structure design, engine selection and fuel consumption estimation.

To study ice resistance of a vessel, there are two main methods, model/full-scale test and numerical model. Both methods have their pros and cons. As for model tests, it has been improved with nowadays advanced model ice and test equipment, hence it is relatively reliable especially when the design ship is very close to some tests. However, at the same time, model test takes too much time and the cost is too high. Thus, the numerical model as a more economical and convenient method plays an important role in ice-worthy ship design, particularly in earlier design stages, even though the results are less precise than real ship/model tests. Based on this, to study numerical models in various ice conditions is worthwhile for ice-going ships. Many researchers have put a lot of effort into building analytical formulae to predict ice resistance since last century, by means of physical analysis, model tests or the combination of both, known as semi-empirical prediction (Vance, 1980; Lewis & Edwards, 1970; Lindqvist, 1989).

1.2 Objectives and goals

The main objective of this thesis is to compare ice resistance models in two ice conditions: broken ice and brash ice. Several kinds of models are selected to predict ice resistance for different ships and compared with the results from experiment data. Since all the semi-empirical models are created for a certain kind of ship or even in a certain kind of ice condition, errors caused by applying them to different ship types are also to be discussed. In addition, various parameters in different models and their influences on the resistance are to be analysed and compared.

The second objective is to study the contribution of ice resistance to the total ship resistance and required power with a ship performance model developed in the project ShipCLEAN; it is hereafter referred to as the ShipCLEAN tool. Also, one certain route is chosen to compare the fuel consumption and sailing time in various ice conditions, which is based on the weather records of 2018.

1.3 Delimitations

In this thesis all the sea ice focuses on the Arctic MIZ, the transition between open water and ice. That is all the sea ice properties are from sites in the Arctic and the sea ice model setting mainly aims to fit the first-year ice in the Arctic region. Depending on the sea ice condition in the MIZ, the main ice types under analysis are broken ice and brash ice.

All the analyses in the case study and route study are limited to no wave, wind, or current speed condition. When required input is lacking for the studied ship (like friction coefficient), the corresponding average value is applied instead, and it will be further explained in the calculation part.

It may be noted that further assumptions and simplifications applied in this thesis are illustrated in the following content.

1.4 Outline of methodology

To illustrate the outline of methodology, in figure 1.2, the flow chart shows the divisions of main part and their focus to study on.

Firstly, sea ice material study is essential for the ice resistance prediction. Based on literature study, different sea ice types and some relevant engineering properties of sea ice are described

in this part. Some kinds of model ice are also reviewed to help to understand their difference and how much it may influence with these ice resistance models and experiment results.

Secondly, various ice resistance models are presented in detail and applied into various case. All the model codes are created in MATLAB® R2010b (The MathWorks Inc, 2010) and evaluated in different cases to study on the usability of each model. The validation of different models is achieved by comparing the results with previous experiment data in various ice conditions.

Finally, ice resistance curves are summarized and sensitivity study for different parameters (like ice density, ice thickness and concentration) is carried out. Based on the recommended ice resistance models from case analysis, the total resistance and required power can be derived from ShipCLEAN tool, also the fuel consumption of a selected route, these results are to be compared with the same situation without ice and discussed to find how much ice could influence on the studied ship in service.

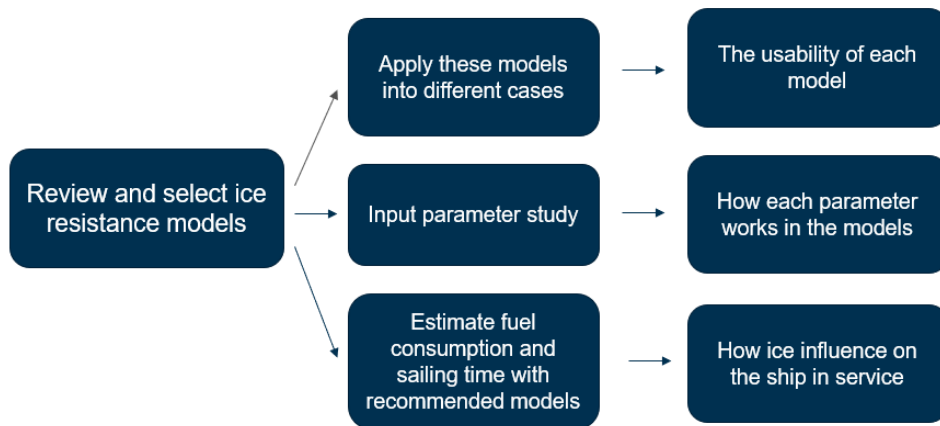


Figure 1.2: Outline of methodology.

2 Sea ice characteristics

The presence of sea ice is clearly the main factor influence the operation and transportation in ice-covered region. However, sea ice is a complex material. It's the freezing form of brine, that means its components might be various from temperatures, regions and other factors. In brief, the components of sea ice can be expressed as: ice + brine + gas + various solid salts. At the same time, each kind of sea ice may have different engineering properties, which affects ice-structure interaction. The purpose of this chapter is to choose suitable ice properties for the simulation afterwards and help to understand how different kinds of sea ice influence with ship ice resistance.

2.1 Difference sea ice types

There are many different divisions of sea ice types, such as age, shape and size and so on. It's quite important to figure out how to define them for the later work. These definitions are mainly based on (Weeks & Hibler, 2010) and (U.S. Department of Commerce,2007). In addition, sea ice is sorted by existing years into two main categories: first year ice and old ice. Ice age leads to a difference in thickness, salinity, density and some mechanical properties.

Table 2.1: Definitions of first-year ice and old ice.

Ice type	Description
First-year ice	Sea ice doesn't grow more than one winter, developing from young ice, with a thickness of 30 cm to ~3 m. It may be subdivided into thin first-year ice (30–70 cm), medium first-year ice (70–120 cm), and thick first-year ice (>120 cm).
Old ice	Sea ice that has survived at least one summer melt season, including second-year ice and multi-year ice.

However, from a practical point of view it is easier to distinguish different types of ice by appearance. In table 2.2, most common ice types in MIZ are introduced.



Figure 2.1: Pancake ice: Circular floes 30 cm - 3 m (1 - 10 ft) across and up to 10 cm (4 in.) thick with raised rims (U.S. Department of Commerce,2007).

Table 2.2: Definitions of ice types divided by appearance.

Ice type	Description
Ice floe	A large sheet of floating sea ice, 20 meters or more across.
Pancake ice	A form of ice in round shape that mostly forms on water covered to some degree in slush, of diameter from 30 centimetres to 3 meters. The name is from this kind of ice looks like a pancake, a signature feature of which is raised edges or ridges on the perimeter, caused by the pancakes bumping into each other from the ocean waves, as it's shown in figure 2.1.
Iceberg	A massive piece of ice of greatly varying shape with a freeboard of more than 5 m that has broken away from a glacier. Icebergs can either be afloat or aground.
Ice ridge	A row of ridge-shaped ice formed by ice under external pressure, like wind or wave.
Level ice	A flat sheet of sea ice that hasn't been affected by deformation. It is a state in which sea ice is not deformed or deformed very small.
Broken ice	It's also called pack ice, that is any sea ice not attached with fixed object, like seafloor, presents in varying sizes, ages, thicknesses and concentrations. It may be caused by icebreakers or melted and separated by a regular seasonal cycle. (an example shown in figure 2.2)
Brash ice	It's relatively small size ice rubble, also called drift ice. Accumulations of floating small fragments (less than 2 m across), the wreckage of other forms of ice (e.g., level ice). Since it mostly appears in ship channel made by icebreaking ships, it is also called channel ice.

As for broken ice, its ice concentration is one weighty parameter, which describes the ratio, in percentage, of the sea surface covered by ice to the total area of the sea surface, both ice-covered (100%) and ice-free (0%) at a specific location or over a defined area. Pre-sawn ice/pre-broken ice is ice sheet that has been pre-cut or pre-broken into pieces, regarded as 100% concentration. Besides, brash ice condition is mostly considered as 100% concentration, since the wreckagees from ice sheet is floating crowdedly within the brash ice channel.

Most Arctic commercial shipping activities happen within the minimum and maximum seasonal limits. Apparently, sea ice appears in the limits, as for ice age, is mostly first-year ice. From a practical point of view, ice resistance modelling study is divided by sea ice appearance (shape and size), as it is easier and clearer for users to define it by visual inspection. Due to the fact that level ice resistance has been studied more than 100 years while other ice conditions are less discussed, this thesis focuses only on broken ice and brash ice condition.

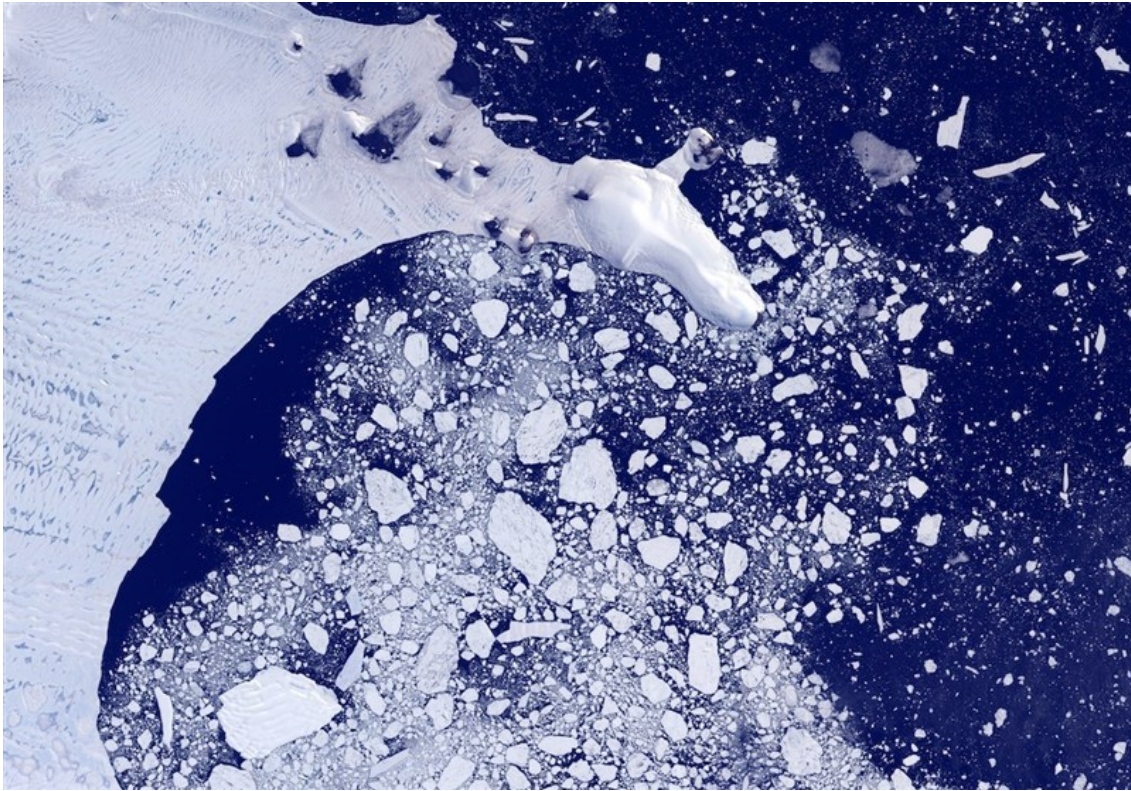


Figure 2.2: Broken ice: West Antarctic Ice Sheet (WAIS) was unstable and collapsing at an accelerating rate due to global warming (Tasnim News Agency, 2019).

2.2 Physical properties of sea ice

The complexity of the mechanical feature of sea ice is decided by its microcosmic construction (salinity, difference of impurity, size of particle and orientation of crystal). Besides, brine and sea ice are various from different regions. In the northern hemisphere, the Baltic sea is less saline than the Arctic sea, since the Baltic is connecting to North Sea with a narrow bay and does not have enough exchange with ocean. (Sun, 2005)

As for floe size of broken ice, it is complicated to ensure its value either in researches or in applications, hence in those ice resistance models, ice floe size is assumed following certain statistical distribution instead of being a variable in equations.

This section introduces several engineering properties of first-year sea ice, more specifically, from sites in the Arctic fields: ice thickness, ice salinity and porosity, ice density and temperature, and ice friction angle.

In the Arctic marginal ice zone, sea surface is mostly covered by broken ice pieces. As those ice floes are only considered to be moved or displaced in the path other than broken up, flexural failure can almost be neglected (Aboulazm & Muggeridge, 1990). Hence, flexural strength and other mechanical properties are not under consideration in this part.

2.2.1 Ice thickness

Ice thickness is a significant property contributing to its volume and weight, which influence ice loads on offshore structures. However, as the wreckage of ice sheet, brash ice is not typically broken into even thickness and it is the same with broken ice pieces. As two kinds of

sea ice analysed in this thesis are broken from level ice, ice thickness of all these ice floes is assumed to follow the same principles as level ice.

Timco and Weeks (2010) concluded that the Arctic ice thickness is directly controlled by two main factors, air temperature and the freezing time. The expected thickness can be determined by the energy balance of heat between water and ice; taking into consideration the daily temperature change. In the view of thermodynamics of ice growth, they also proposed an equation, simplified from the Stefan equation, to describe sea ice thickness, h_i :

$$h_i = 0.035\alpha[\sum(T_b - T_a)t]^{0.5} \quad (2.1)$$

where α is a factor to take the snow cover, wind speed and the ocean heat flux effects into account, always less than one, and varies for regions; T_b and T_a are the temperatures at the bottom and top of the ice respectively, and T_a is also considered as the ambient air temperature. In addition, the sum describes each time period of ice growing in varying temperatures and t is the freezing time in days.

2.2.2 Ice salinity and porosity

Ice salinity and porosity are two significant factors, correspondingly influencing the mass and volume of sea ice. The former one describes the weight of salt in a certain mass of sea ice and another one defines the amount of gas per unit volume. The average ice salinity (S_i) is found to be related with ice thickness (Kovas, 1996)

$$S_i = 4.606 + [91.603/h_i] \quad (2.2)$$

where S_i is the salt weight in grams per kilogram sea water, usually in the unit of ppt or ‰ ; h_i is ice thickness in cm.

Inside sea ice rubbles, brine also takes an important portion and its volume (in parts per thousand), v_b is dependent on the ice temperature(T) and salinity. It can be determined by Frankenstein and Garner equation:

$$v_b = S_i \left(\frac{49.185}{|T|} + 0.532 \right) \quad (2.3)$$

where $-0.5^\circ\text{C} \geq T \geq -22.9^\circ\text{C}$. Another important part in porosity is the relative gas or air volume in the ice v_a . (Cox & Weeks, 1983) Air volume in ice is usually determined by measuring the mass and volume of the ice at a certain temperature and the mass of salts and water from the melted sample. The total ice porosity is expressed as the sum of the relative volume of brine and gas:

$$v_T = v_b + v_a \quad (2.4)$$

2.2.3 Ice density and temperature

The density of ice is one of the most important engineering properties to determine the weight of a certain ice block. In addition, the density difference between sea ice and water is dominant of buoyancy force during ship ice-resistance estimation, since ice floes are submerged into sea water.

Sea ice density values present a quite wide range, which can be sorted into two categories: ice above the waterline and ice below the waterline. Accurate tests show that the density of the

first form varies from 840 kg/m³ to 910 kg/m³ and 900 kg/m³ to 940 kg/m³ for another (Weeks & Hibler, 2010).

Figure 2.3 is the result computed from the Cox and Weeks (1983) equations, describing the gas-free sea ice densities at different temperatures and salinities. Lines in the figure can be considered as the maximum sea ice density limit in each case. All the ice density estimates discussed above are only for the gas-free first-year sea ice and Weeks and Hibler suggested that 920 kg/m³ could be a reasonable value for most engineering application. However, the presence of ice porosity especially the gas porosity causes the actual sea ice densities always lower than the predicted values.

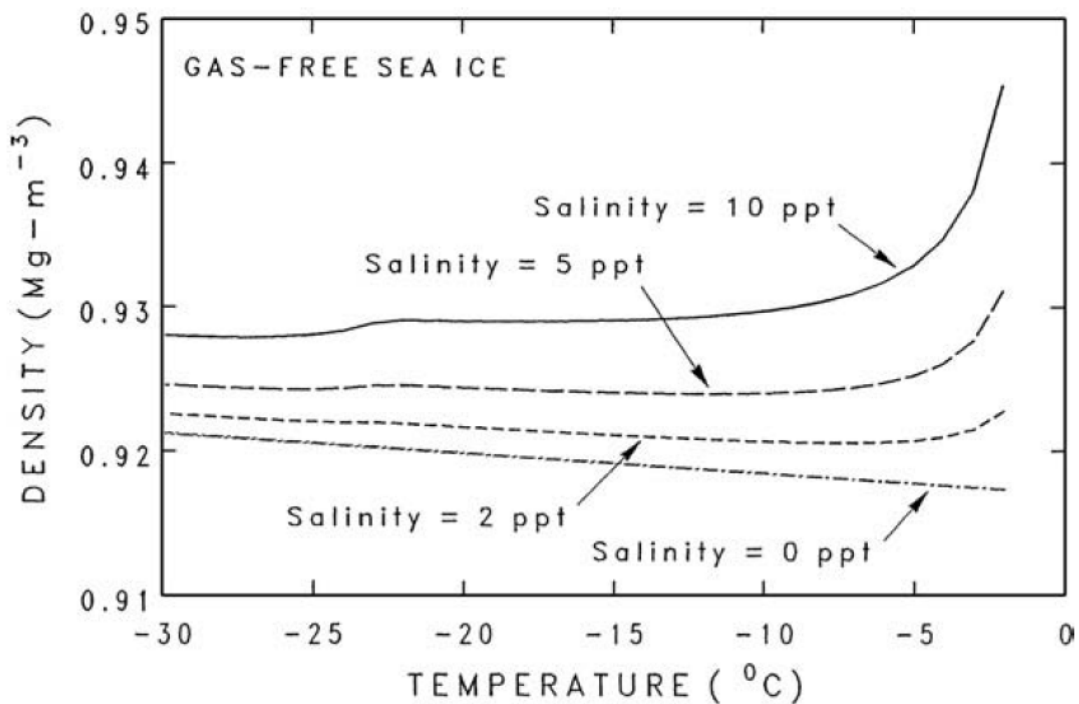


Figure 2.3: Plot of the density versus temperature for four different salinities for gas-free sea ice. (Weeks & Hibler, 2010).

2.2.4 Friction angle

The Mohr-Coulomb yield criterion is widely recommended to describe the shear resistance of brash ice by ISO/FDIS/19906 (2010). In ship resistance analysis, the concern of sea ice deformation also follows the Mohr-Coulomb criterion, which introduces the definition of friction angle ϕ (also called angle of shear resistance) in plane strain conditions:

$$\sin\phi = \frac{\sigma_1 - \sigma_3}{\sigma_1 + \sigma_3} = \frac{t}{s} \quad (2.5)$$

where t is maximum shear stress and s is mean stress in the shearing plane, computed by equations 2.6 and 2.7; σ_1 and σ_3 are major and minor stresses.

$$t = \frac{\sigma_1 - \sigma_3}{2} \quad (2.6)$$

$$s = \frac{\sigma_1 + \sigma_3}{2} \quad (2.7)$$

A linear relationship between shear stress and mean stress can be determined in bi-axial compression tests, that is the friction angle is constant, except for the beginning unstable stage (Kulyakhtin & Høyland, 2015). Besides, range of friction angles from 31° to 66° is required by the application of this criterion.

2.3 Previous ice models

During ice-related tests, ensuring environment temperature is always an issue to overcome. In this case, ice models came into use instead of real ice and these could lead to some errors in the experiments. This part is to introduce the properties of different ice models and how these might influence with the results and conclusions. All the information about ice models in this section is based on the reviews of (Lau, et al., 2007).

In order to minimize the requirements of experimental facilities and reduce costs, in 1955 model ice was first introduced into use by the Arctic and Antarctic Research Institute (AARI) in Russia. It was made from 3% sodium chloride solution and simulated the growth of true sea ice to obtain a similar crystal structure. This method was later widely used in many countries, such as Germany and Finland. Later, saline model ice was improved by Evers and Jochmann (1993) and is still applied in HSVA (Hamburg Ship Model Basin).

In 1979, Timco investigated a new kind of model ice made of 1.3% carbamide solution. This urea ice performs better in both strength and rigidity characteristics than the saline ice. EG/AD/S ice is another common ice model grown from the solution of ethylene glycol, aliphatic detergent, and sugar. Since brittle performance of saline ice is not scaled properly when scale factor more than 30, EG/AD/S ice was found to be superior than saline model ice and urea model ice (Timco, 1986). It was improved by Spencer and Timco (1990) to achieve a better density by compressing bubbles inside EG/AD/S ice and called Correct Density-EG/AD/S (CD-EG/AD/S), which is also the main kind of ice model used in the ice tank of IOT (Institute for Ocean Technology, Canada).

Many unrefrigerated ice models made of paraffin wax, plaster, or other mixtures are also used in towing tank to perform ship resistance experiments without breaking force, such as in pack ice condition. In 1964, Corlett and Snaith (1964) first introduced paraffin as model ice by for performing model-scale resistance experiments. Based on the statistical values of Bohai ice physical and mechanical properties, DUT-1, a mixture of polypropylene, white cement and water was developed for the model ice experiments at room temperature (Li, et al., 2000) and it is applied into use in Dalian University of Technology.

Most studied ice resistance models in the chapter 3 and also cases in chapter 4 are concluded from experiments in ice tank or even normal towing tank. Hence, some shortcomings of model ice application might influence their results and conclusion.

3 Ice resistance models

A lot of research and studies have been done on sea ice mechanics and ice loads on ships and there are many existing theoretical or semi-empirical models of ice resistance study (Enkvist, 1972; Su, et al., 2010; Pernas Sánchez, et al., 2012; Paavilainen, 2012).

Conventionally, the primary research on ice-going ships focuses more on the prediction of their performance under level ice condition (Lindqvist, 1989; Riska, et al., 1997; Myland & Ehlers 2018). However, brash ice and broken ice, as the main sea ice types in the Arctic MIZ, are relatively under less investigation.

In this part, various ice resistance models in broken ice and brash ice (also called channel ice) conditions are to be introduced and compared in detail. It should be noted that some of the following models simulate the total resistance while others only have ice resistance; only the resistance from ice in each model will be applied into computation and ShipCLEAN tool. Each ice resistance model is called after the authors' name in this thesis.

3.1 Broken ice

Compared to level ice and brash ice, broken ice resistance prediction is a quite new field for researchers and standardization in pack ice testing analysis has not yet developed. Colbourne (2000) presents the total ice resistance consists of two components, open-water resistance and pack ice resistance. Besides, each follows a separate scaling law.

Then Colbourne introduced a pack ice Froude number (C_p) and force coefficients based on non-dimensional methodology for scaling and analysing model tests of ship ice resistance in pack ice condition. Following this analytical method, Guo et al. (2018), Woolgar and Colbourne (2010) presented semi-empirical models for different ship types.

3.1.1 The Guo model

Based on Colbourne's theoretical analysis, Guo et al. (2018) designed a model test for KCS, which was made in a towing tank and paraffin was used to simulate sea ice. From the experiment, the scale factor, λ is 52.667. To ensure the stability of ice properties, a kind of synthetic model ice is applied to simulate sea ice pieces. An average ice-hull friction coefficient is taken as 0.035 in this model test.

As for the open-water component, it follows Reynolds scaling and including a form effect introduced by Prohaska (SNAME, 1988). It is rational when the speeds are low enough to neglect the wave resistance component. Before scaling, open-water resistance is shown as, (Guo, et al., 2018)

$$R_{OW} = C_{OW} V_m^2 = 6.817 * V_m^2 \quad (3.1)$$

As the experiment was made in a towing tank, it is assumed to take place at room temperature 15°C. Based on ITTC, the kinematic viscosity of 15°C fresh water is 1.1386E-06 m²/s, and 0°C sea water is 1.8480E-06 m²/s. (ITTC, 2011) The viscous resistance scaling follows the same scaling method with friction resistance and the scale between model ship and full-scale ship is,

$$scale = \frac{C_{OWs}}{C_{OWm}} = \frac{(1+k)C_{fs}*\lambda^2}{(1+k)C_{fm}} = \frac{(1+k)*0.075/(\log_{10}Res-2)^2*\lambda^2}{(1+k)*0.075/(\log_{10}Rem-2)^2} \quad (3.2)$$

Colbourne and Lever(1992) presented an analysis that since C_{OW} , which represents for $\frac{1}{2}\rho_w S$ (ρ_w is sea water density, S is wet surface area), is not completely non-dimensional, to eliminate dimensional effects from S , R_{OW} is scaled by λ^2 additionally. Open-water resistance for full scale ship is,

$$R_{OW} = C_{OW}V_s^2 = 6.817 * Vs^2 * scale \quad (3.3)$$

In addition, pack ice Froude number, Fr_p and pack ice force coefficient, C_p are introduced as equations (3.4-3.5).

$$Fr_p = V/\sqrt{gh_i C} \quad (3.4)$$

$$R_p = C_p \rho_i B h_i V^2 C^n \quad (3.5)$$

Here, $n=3$ is recommended by Colbourne for moored ships and FPSOs, but later $n=2$ is found to be more suitable for the Arctic tankers (Molyneux & Kim, 2007). Besides, Colbourne found Fr_p have a linear ln-ln relationship with C_p . Guo et al. concluded from experiment results that pack ice force coefficient is,

$$C_p = 4.4Fr_p^{-0.8267} \quad (3.6)$$

After all, total resistance for the full ship in broken ice is derived as,

$$R_T = R_{OW} + R_p = 6.817V^2 * scale + 4.4Fr_p^{-0.8267} \rho_i B h_i V^2 C^2 \quad (3.7)$$

where V is ship speed in m/s, ρ_i is ice density in kg/m^3 , B is ship beam in m, h_i is ice thickness in m, C is ice concentration.

3.1.2 The Woolgar and Colbourne model

After pack ice Froude number C_p was introduced in pack ice resistance analysis, Woolgar and Colbourne (2010) continued to further investigate how the independent variables affect the estimate of C_p . Based on the experiment data from the stock tanker and the FPSO, they determined a set of prediction constants for these two kinds of vessels. To make clear the influence from each factor, C_p is expressed as (Woolgar & Colbourne, 2010)

$$C_p = 10^a (Fr_p)^b C^c (f)^d \quad (3.8)$$

where Fr_p is pack ice Froude number, C is ice concentration, f is hull-ice friction coefficient and a - d are the regression coefficients for each variable, shown in table 3.1.

Table 3.1: Prediction constants (Woolgar & Colbourne, 2010).

Variable	Constant	Coefficient- Stock Tanker	Coefficient- FPSO
Regression intercept	a	1.224	1.872
Fr_p	b	-1.761	-1.513
C	c	3.866	4.447
f	d	0.265	0.265

All the constants are predicted from the previous tests and show the influences from different ship types. FPSO is designed to float over sea surface as an oil storage with blunt bow and stern and also big block coefficient. From the constant coefficients in table 3.1, it can be found that

FPSO is more affected by ice concentration and a little bit less affected by the speed comparing to stock tankers. With C_p is known, pack ice resistance can be computed by:

$$R_p = \frac{1}{2}C_p\rho_i B h_i V^2 C^3 \quad (3.9)$$

Here the exponent of concentration still equals to 3 instead of changing to the suggestion of 2 from Molyneux and Kim (2007). However, in this thesis, the focus is on commercial ice-going vessels, hence, in the following part only the formula concluded from stock tanker is applied and analysed.

3.2 Brash ice

Operating in the brash ice channels is the most common mode for commercial vessels. They only need to navigate in the existing old route filled with ice wreckages. In this part, two brash ice models from Riska et al. (1997) and Mellor (1980) are presented. Besides, Spencer and Jones (2010) concluded a pre-sawn ice resistance formula from the data of medium R-class icebreaker model tests.

3.2.1 The Spencer and Jones model

From IMD standard method of analysis, the total ice resistance, R_T is divided into four components: open water resistance, R_{OW} , ice buoyancy resistance, R_B , ice clearing resistance, R_C , and ice breaking resistance, R_{BR} . Based on it, the pre-sawn ice resistance, R_{pr} is derived by excluding the breaking component out of the whole resistance (Spencer & Jones, 2001)

$$R_{pr} = R_{OW} + R_B + R_C \quad (3.10)$$

Hence, Spencer and Jones tried to create a simple numerical formula to predict ice resistance from the model tests at the Institute for Marine Dynamics and full-scale tests of three R-class icebreakers. The required input is B , T , V , h_i (ice thickness) and ice-hull friction condition (depending on the painting condition and corrosion effect) between the analysed ship and ice, and $\Delta\rho$ (the difference in density between water and ice).

In this set of experiments, they used concept of ice-hull friction coefficient to scale the friction resistance between full scale and model scale. The range of ice-hull friction coefficient, measured by previous researchers (Mäkinen, et al., 1994) is quite large from 0.01 to 0.6. Hence, two models of ice-hull friction coefficient 0.09 and 0.03 was chosen to represent the high friction model and low friction model respectively. During the model tests, models were towed in open water and pre-sawn ice (in IMD ice tank) separately.

Open water resistance is assumed to be the same with different friction conditions. Hence, its equation is simply concluded from open-water test of low friction model and only suitable for full-scale ships less than 9 knots: (Spencer & Jones, 2001)

$$R_{OW} = 14.6 * V^2 \quad (3.11)$$

Here the open-water resistance could be scaled in the same way with equations (3.1-3.3), while the scale factor, λ is 20.

Ice buoyancy resistance is the only component assumed to be independent of speed, which is from the buoyancy against ice.

$$R_B = C_B \Delta\rho g h_i B T \quad (3.12)$$

where C_B is a nondimensional coefficient of buoyancy resistance (concluded from model test $C_B=1.31$ for low friction, $C_B=2.67$ for high friction), g is standard gravity.

Ice clearing is derived from model tests and concluded as nondimensional coefficients C_C ,

$$C_C = \frac{R_C}{\rho_i B h_i V^2}; \quad (3.13)$$

where C_C is the coefficient of the clearing resistance, and ρ_i is the density of ice.

During the analysis, ship speed is made to be dimensionless by using ice Froude number (F_h) where the ice thickness as its characteristic length, defined as,

$$F_h = \frac{V}{\sqrt{g h_i}} \quad (3.14)$$

A linear relationship in ln-ln scale was found between ice Froude number and clearing coefficient. Then the clearing resistance for the low and high friction cases (Spencer & Jones, 2001):

$$R_C = 0.90 F_h^{-0.739} \rho_i B h_i V^2 \quad (3.15)$$

$$R_C = 2.03 F_h^{-0.971} \rho_i B h_i V^2 \quad (3.16)$$

To sum up, the total brash ice resistance can be expressed as,

$$R_i = 0.90 F_h^{-0.739} \rho_i B h_i V^2 + 1.31 \Delta \rho g h_i B T \quad (3.17)$$

$$R_i = 2.03 F_h^{-0.971} \rho_i B h_i V^2 + 2.67 \Delta \rho g h_i B T \quad (3.18)$$

Equations (3.8) and (3.9) give the total brash ice resistance for low and high friction ships respectively. From the formulae, it can be found that ice resistance with high friction almost twice than low friction condition. However, ice-hull friction coefficient of 0.09 is relatively high in steel vessels and 0.05 is the best friction coefficient suggested by Lau (2018) that a new hull in snow free condition can achieve, which is within the range of two models and closer to the low friction one. Based on this, in the following part, only the lower ice-hull friction formula is discussed and compared.

3.2.2 The Riska model

The most common navigation condition for merchant vessels is to follow an old channel or be assisted with an icebreaker. Ice resistance formula presented by Riska et al. (1997) was designed for merchant vessels in channel ice condition in the Baltic sea. It is also included in the Finnish-Swedish Ice Class Rules. This method is based on ten commercial vessels' full-scale trials and contains a lot of empirical constants. In this method, ice resistance measurement is based on the assumption (Riska, et al., 1997):

$$R_T = R_{OW} + R_i \quad (3.19)$$

Since open-water resistance is usually very small compared to the ice resistance part, the coupling between them is neglected during the analysis. Besides, hydrodynamic resistance estimation is quite mature hence only ice-related component is presented in this method. Based on soil mechanics and Mohr-Coulomb failure criteria, an entirely analytical formula for channel ice resistance with speed dependency was created as (Riska, et al., 1997):

$$R_{CH} = \frac{1}{2} * \mu_B * \rho_\Delta * g * h_F^2 * K_p * \left[\frac{1}{2} + \frac{h_M}{2h_F} \right]^2 * \left[B + 2 * h_F * \left(\cos\delta - \frac{1}{\tan\Psi} \right) \right] * (\mu_h * \cos\beta + \sin\Psi * \sin\alpha) + \mu_B * \rho_\Delta * g * K_0 * \mu_h * L_{par} h_F^2 + \rho_\Delta * g * \left[\frac{L*T}{B^2} \right]^3 * h_M * A_{WF} * Fn^2 \quad (3.20)$$

where μ_B is $(1 - p)$ (p is ice porosity, $p = 0.1-0.2$), ρ_Δ is the density difference between water and ice, μ_h is the friction coefficient between ice and hull. h_M is the thickness of the brash ice in the middle of the channel, h_F describes the thickness of brash ice layer on the side (see figure 3.1). As for ship details, L_{par} , A_{WF} , α , β are parallel body length, foreship waterline area, waterline entrance angle, the angle between the waterline and the vertical at $B/2$ respectively and Fn is the Froude number. g is gravity constant, K_p is the coefficient of passive stress, K_0 is the coefficient of lateral stress at rest. Here, h_M represents the ice thickness of the brash ice, which is written as h_i in other models.

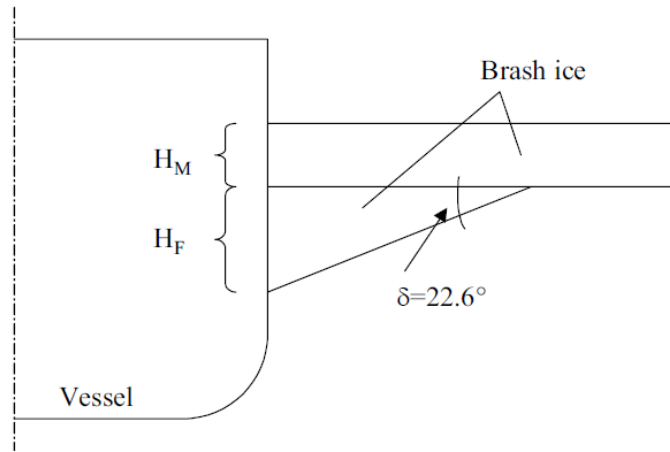


Figure 3.1: Definitions for h_M , h_F and δ (Juva & Riska, 2002).

To further simplify the brash ice resistance model, L_{par} , A_{WF} , ϕ , α are assumed to be related to the main dimensions L , B , T according to average or conservative relationships ($L_{par} = 0.45L$, $A_{WF} = 0.25LB$, $\alpha = 30^\circ$, $\phi = 40^\circ$) (Juva & Riska, 2002). The equation was originally simplified to be independent on ship speed and only suitable for the low speed (less than 5 knots). After a deep understanding of physical meaning in each term, the last term in the simplified equation is replaced by the speed-related component in equation (3.18). The resistance is shown as follows:

$$R_i = C_1 + C_2 + C_3[H_F + H_M]^2[B + 0.658H_F] + C_4LH_F^2 + \rho_\Delta * g * \left[\frac{L*T}{B^2} \right]^3 * H_M * A_{WF} * Fn^2 \quad (3.21)$$

Where:

$$C_1 = f_1 \frac{BL}{2T^{+1}} + 1.84 * (f_2B + f_3L + f_4BL) \quad (3.22)$$

$$C_2 = 3.52 * (g_1 + g_2B) + g_3 \left(1 + 1.2 \frac{T}{B} \right) \frac{B^2}{\sqrt{L}} \quad (3.23)$$

for ships in ice class IAS without a bulb or

$$C_1 = f_1 \frac{BL}{\frac{2T}{B}+1} + 2.89 * (f_2B + f_3L + f_4BL) \quad (3.24)$$

$$C_2 = 6.67 * (g_1 + g_2B) + g_3(1 + 1.2 \frac{T}{B}) \frac{B^2}{\sqrt{L}} \quad (3.25)$$

for ships in ice class IAS with a bulb or C_1 and C_2 both are zero in other ice classes.

$$H_F = 0.26 + (H_M * B)^{0.5} \quad (3.26)$$

Apart from that, the term $\left[\frac{L*T}{B^2}\right]^3$ should be taken as 20 if it is above 20 or 5 if it is lower than 5. Besides, other constant coefficients are shown in table 3.2.

Table 3.2: The constants in the formulae for brash ice resistance (Riska et al. 1997).

$f_1=10.35\text{kN/m}^2$	$g_1=1537.3\text{N}$	$C_3 = 459.993 \text{ kg}/(\text{m}^2\text{s}^2)$
$f_2=45.8\text{kN/m}$	$g_2=172.3\text{N/m}$	$C_4 = 18.783 \text{ kg}/(\text{m}^2\text{s}^2)$
$f_3=2.94\text{kN/m}$	$g_3=398.7\text{N/m}^{1.5}$	
$f_4=5.8\text{kN/m}^2$		

3.2.3 The Mellor model

Mellor (1980) developed an entirely analytical equation of ship ice resistance prediction by assuming a linear Mohr-Coulomb failure criterion in brash ice. This study focuses on low speed ships and the emphasis is on the resistance of bow. In the analysis, brash ice resistance consists of bow resistance and frictional hull resistance after the bow. By summing these two components total ice resistance can be estimated for sharp bow and blunt bow respectively (Mellor, 1980)

$$R_i = (1 + 2\mu_e(k_1 + k_2N))BR = A_1BR \quad (3.27)$$

$$R_i = (1 + \tan\phi \cot\beta'' + 2\mu_e k_2N)BR = A_2BR \quad (3.28)$$

R represents the resistance force per unit width,

$$R = \frac{1}{2} \left(\frac{1+\sin\phi}{1-\sin\phi} \right) (1 - n)\rho_i g (1 - \rho_i/\rho_w) h_i^2 \quad (3.29)$$

where ρ_i, ρ_w are ice and water densities, h_i is ice thickness, ϕ is the angle of shear resistance, β'' is the apex half-angle of the wedge shape, μ_e is effective friction coefficient, and N is an uncertain factor taken as 0.1. k_1 and k_2 are the ratio of the bow section length(L_1) and parallel body length(L_2) to the beam. These parameters are further explained in figure 3.2.

Mellor also found that the numerical values of A_1 mostly within the range of 1.3 to 2.5 and A_2 in the range of 1.7 to 2.6. Both are dominated by the hull geometry and friction.

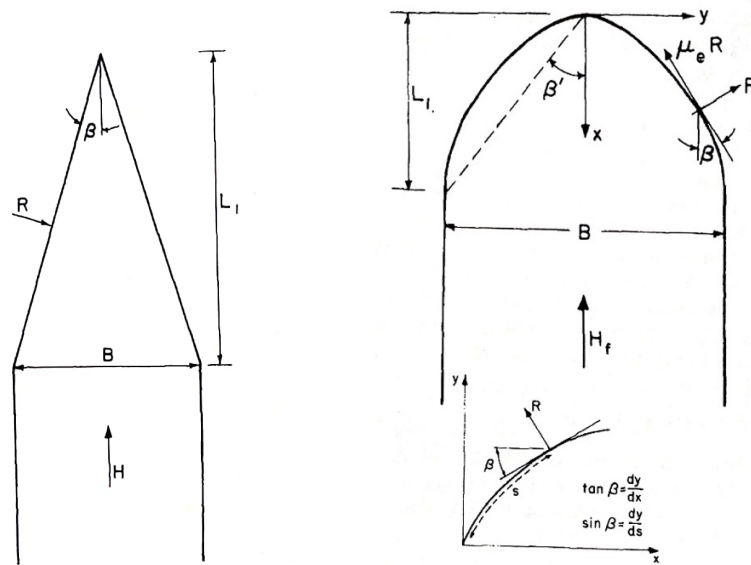


Figure 3.2: Plan diagrams of a wedge bow (left) and a blunt bow (right) pushing horizontally into brash ice (Mellor, 1980).

3.3 Model summary

Broken ice and brash ice are quite similar conditions, since in both cases there is no icebreaking force involved, which is the main part (between 40%-80% of total resistance) in level ice condition (Enkvist, 1983). The difference between is that broken ice includes massive ice pieces in various shapes and distributed sparsely while brash ice only contains small ice floes but might have side effect from the canal width limit. Hence, all the studied models will be compared together.

It should be noted that some of these models get the total resistance (Guo, et al., 2018; Spencer & Jones, 2010) while others only focus on the ice resistance (Woolgar & Colbourne, 2010; Riska, et al., 1997; Mellor, 1980). Since only net ice resistance is required in this thesis, open water component in the Guo model and the Spencer and Jones model is excluded in the following part. In addition, the Mellor model is completely derived in analytical way and no empirical part is included in this method.

It could be concluded that total ice resistance in brash ice condition is consisting of two main components, one is independent from ship speed, which comes from submersion ice pieces and other one is almost linearly proportional to V^2 in a certain condition. In very low ship speed, the ice buoyancy resistance is dominating, and the speed-related term is quite low relative to it. As for broken ice condition in Colbourne's analytical method, ice pieces without side effect tend to move around instead of being submerged, hence give less buoyancy resistance to ship hull.

Here is a short comparison among different models shown in table 3.3. The weight of ice has a great influence in ice resistance as ice thickness and density are two necessary factors for all the models. The density difference between water and ice is also essential for the ice buoyancy resistance part in brash ice models. Additionally, ice concentration also makes a contribution to broken ice resistance.

Ice-hull friction is also taken into account in most models. It is dependent on several parameters, including painting condition of ship hull and sea ice temperature, surface roughness. To describe the friction of various vessels, ice-hull friction coefficient is introduced instead in order to neglect the scale influence. In the terms of required ship details, ship beam is the only essential information since other geometry factors are assumed to be related to the beam and included in the empirical part, while ship length is the least used one. Besides, it can be found that the bow section, both shape and length, has an impact on the ice resistance. Table 3.3 also presents the ship types they focused on during the analysis and model/ full-scale ship tests. Except the model from Spencer and Jones is designed for icebreakers, others are designed for commercial ice-going ships.

Table 3.3: Comparison among different models.

Ice type		Broken ice		Brash ice		
		Guo, et al. (2018)	Woolgar (2010)	Spencer & Jones (2001)	Riska, et al. (1997)	Mellor (1980)
Ice-related variables	model ice region	model ice	Canada's ice basin model	Canada's ice basin model	first-year Baltic Sea ice	Arctic ice
	ice thickness	h_i	h_i	H_i	H_M	h
	porosity				n	n
	ice density	ρ_i	ρ_i			ρ_i
	density difference			$\Delta\rho$		$\Delta\rho$
	friction angle					ϕ
	concentration	C	C			
ship details	ship type	KCS	stock tanker/ FPSO	R-Class icebreaker	merchant ship	
	speed	v	v	v	v	
	length				L	
	length of bow					L_1
	parallel mid-body length					L_2
	beam	B	B	B	B	B
	draught			T	T	
	ice-hull friction		f	high (or low)		μ_e
	apex half-angle					β
	bow shape				bulb (or not)	sharp (or blunt)
	Ice Class				IAS (or etc.)	

4 Description of case study

After the model study in chapter 3, all the models are coded in MATLAB for case applications. Section 3.3 states that all the studied models are created to be specific to a certain type of vessels and their adaptability for other ship types is also worthy of assessment.

In this section, three groups of experiment results from various ship types and ice conditions are compared with the created models. The experiment data in each case is respectively collected from Molyneux and Kim (2007), Kim, et al. (2018), Hu and Zhou (2016). Table 4.1 summarizes the focused ship types and ice types in each case.

Table 4.1: Summary of the studied cases.

	Case 1		Case 2	Case 3
Ship type	Ice-breaking tanker	Traditional tanker	Icebreaker-Araon	Ice-breaking tanker
Broken ice	×	×	×	
Brash ice			×	×

All the models are compared by the error of each estimate, which is computed as the ratio in equation 4.1 in order to assess the fit of each prediction.

$$Error = \frac{model\ prediction\ value - Experiment\ value}{Experiment\ value} \times 100\% \quad (4.1)$$

4.1 Input values

Due to the observational limitations in actual navigation, only ice thickness and concentration are variable inputs during the whole simulation.

Because of time limit, all other ice related factors are assumed to be constant in this thesis, except for the values mentioned in certain case. These values shown in table 4.2 are based on the review work in sections 2.2 and 2.3.

Table 4.2: Input values for the calculations in the thesis.

Properties	Unit	Input values
Ice density	kg/m ³	900
Sea water density	kg/m ³	1250
Ice porosity	-	0.15
Friction angle	deg	50

4.2 Comparison for Case 1

With potential development of oil and gas transportation in the Arctic and Baltic region, large oil tanker's performance in ice is of higher interest. There are four icebreaking tanker models, IMD 493, IMD 501, IMD 614, IOT 648 and a conventional tanker, SM-173, built by Samsung Heavy Industries. Table 4.3 shows bow shapes and main principle dimensions of these test models.

Molyneux and Kim (2007) did a set of model test with these five tankers in broken ice condition, where ice was set in the thickness of 0.75m with 95% concentration. All the models were towed

in IOT ice tank in St. John's, Newfoundland, Canada and CD-EG/AD/S model ice was used to simulate real sea ice.

Table 4.3: Principal particulars of the tested models.

Model number	IMD493	IMD501	IMD614	IOT618	SM-173
Design	Aframax Arctic	Aframax Arctic	Suezmax Arctic	Suezmax Baltic	Suezmax No ice
Bow shape	R-Class#1	R-Class#2	Spoon	Ice bulb	Bulb
Length[m]	273.5	274.9	284.0	271.48	258.3
B[m]	43.6	43.6	42.8	44	46.2
T[m]	11.5	11.5	16.5	15	16.6
Model scale	31.94	31.94	33.87	36.82	44.5

In Case 1, for the reason that all the experiment results only present their total resistances, open-water resistance is assumed to be the same in two models and it is computed by following the Guo model formulae, that is equations 3.1-3.3. Without knowing ice-hull friction coefficients, an average value of 0.13, recommended by Woolgar and Colbourne (2010) is assumed for all the models.

The test results and estimated results are presented in figure 4.1-4.2 and Appendix A. Both the Guo model and the Woolgar model are simulated with the same variables as the model tests. Since ship geometry in both models is already assumed to be related with ship beam, there is no big gaps of resistance difference among the estimates for different ships. Predicted resistance from semi-empirical models grows with speed in a quite smooth and similar trend, while the data of different test ships grows variously.

After the estimates from models are known, all the estimated errors in case 1 can be derived by equation 4.1 and the results are shown in table 4.4. It is clear to find that the maximum error is 60% in the Guo model and 66% in the Woolgar and Colbourne model. Besides, the average errors show that the first model overestimates the resistance 1% while the second model underestimates the resistance 25% in this case, and from the standard deviations it could be found that the Guo model is more widely distributed.

Both models predict better for the icebreaking tankers (see figure 4.2) than the conventional one (see figure 4.1), while they underestimate most situations more than 50% of the actual total resistance.

Table 4.4: Pack ice resistance comparison between studied models and model tests.

Speed	Error [%] - The Guo model				Error [%] - The Woolgar and Colbourne model			
	4.8knots	5.8knots	6.8knots	7.8knots	4.8knots	5.8knots	6.8knots	7.8knots
IMD-493	0.12	12.34	23.15	32.86	-7.36	-11.57	-14.88	-17.43
IMD-501	6.80	26.38	35.32	32.86	-1.19	-0.52	-6.46	-17.43
IMD-614	21.10	32.51	34.52	30.64	12.05	4.34	-6.96	-18.73
IMD-648	-29.75	-18.42	-8.01	-1.75	-35.00	-35.80	-36.43	-38.97
SM-173	-60.28	-54.59	-49.25	-44.77	-63.26	-64.29	-64.99	-65.78
Average	1.09				-24.53			
Standard deviation	33.70				24.74			

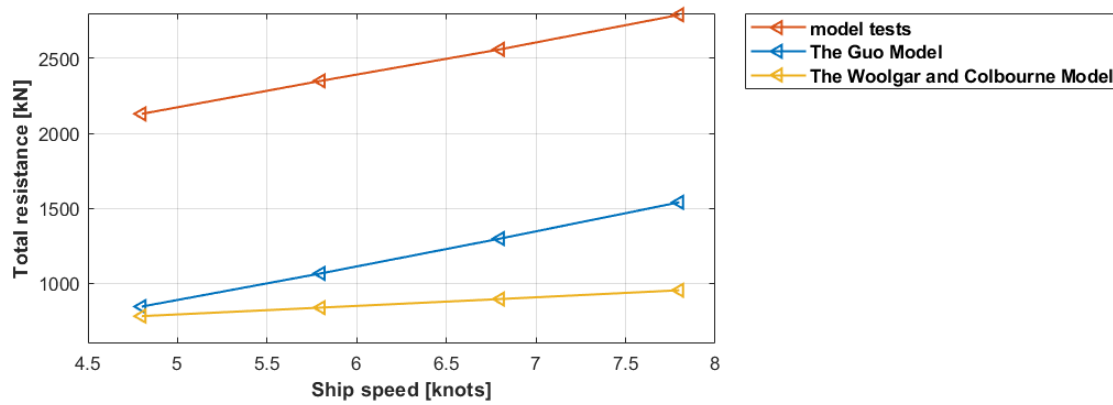


Figure 4.1: Total ice resistance comparison between studied models and model tests in 0.75m thickness pack ice (95%) for conventional tanker.

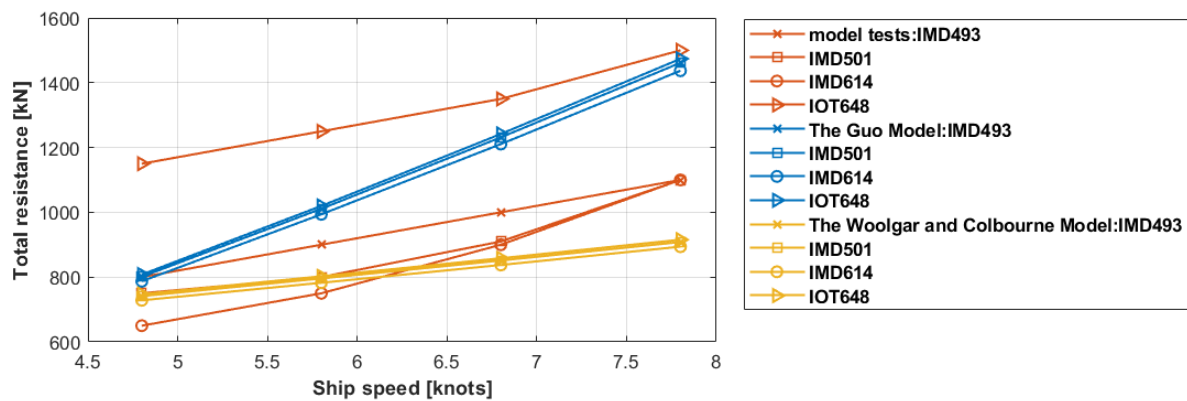


Figure 4.2: Total ice resistance comparison between studied models and model tests in 0.75m thickness pack ice (95%) for icebreaking tankers.

4.3 Comparison for Case 2

Kim, et al. (2018) designed a set of experiment for the icebreaker RV Araon to study on its performance in various ice conditions. The model test using RV Araon model was performed in broken ice of 1.06m thickness in concentrations of 60%, 80% and 90% and in 0.86 m thickness brush ice. RV Araon is a large icebreaker designed in South Korea and the particulars of the full-scale ship are presented in table 4.5.

Table 4.5: Principal particulars of the ARAON (Kim, et al., 2011).

Length, O. A. [m]	Length, B.P. [m]	Beam [m]	Draft [m]	Model scale
111	95	19	6.8	18.67

Since the experiment data is total resistance, in the predictions of studied ice resistance models the open-water resistance is computed by using the Spencer and Jones model (eq. 3.11) as their model was concluded from R-class icebreakers which is closed to RV Araon in ship shape and dimensions. Values of the model estimates and experiment data are attached in Appendix A and figures 4.3-4.4. In order to compare the adaptability of different models, their errors are also calculated by equation 4.1 and results are shown in tables 4.6-4.7.

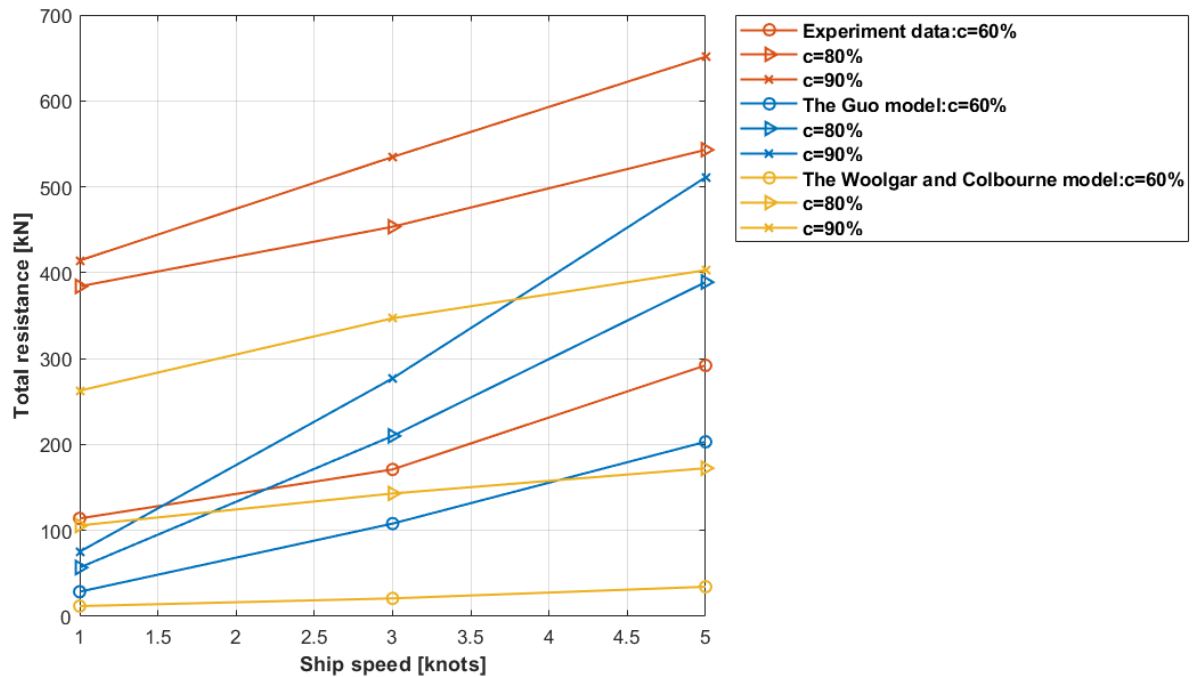


Figure 4.3: The comparison between model estimations with RV Araon model test in 1.06m thickness broken ice condition.

Table 4.6: Broken ice resistance comparison between studied models and model tests.

Speed	Error [%] - The Guo model			Error [%] - The Woolgar and Colbourne model		
	1 knot	3 knots	5 knots	1 knot	3 knots	5 knots
C = 60%	-74.84	-36.85	-30.43	-89.51	-87.76	-88.20
C = 80%	-85.21	-53.68	-28.37	-72.44	-68.46	-68.25
C = 90%	-81.83	-48.19	-21.54	-36.57	-35.11	-38.15
Average	-51.21			-64.94		
Standard deviation	24.26			22.79		

In broken ice condition, various ice concentrations were carried out in the experiments. Both models predict quite different results from the experiment data, where the difference between them varies from -30% to -90%. The Guo model shows larger errors in low speed and the maximum error -85% presents at 1 knot ship speed in 80% ice concentration. The Woolgar and Colbourne model estimations are more different from the test results at lower concentrations and the worst of estimate is -90% at 1 knot ship speed in 60% ice concentration.

Overall, the Guo model performs a little bit better than the Woolgar and Colbourne model in this case even with a slightly more standard deviation. In the Mellor model, there are some unknown required variables and the average values concluded from Kitazawa and Ettema (1985) and Jones (1989) are applied during the estimation: in the equation for blunt bow, the ratio between the parallel body and beam is 8; the effective ice-hull friction coefficient is 0.20. In the Riska model, the ice class is applied other than IAS.

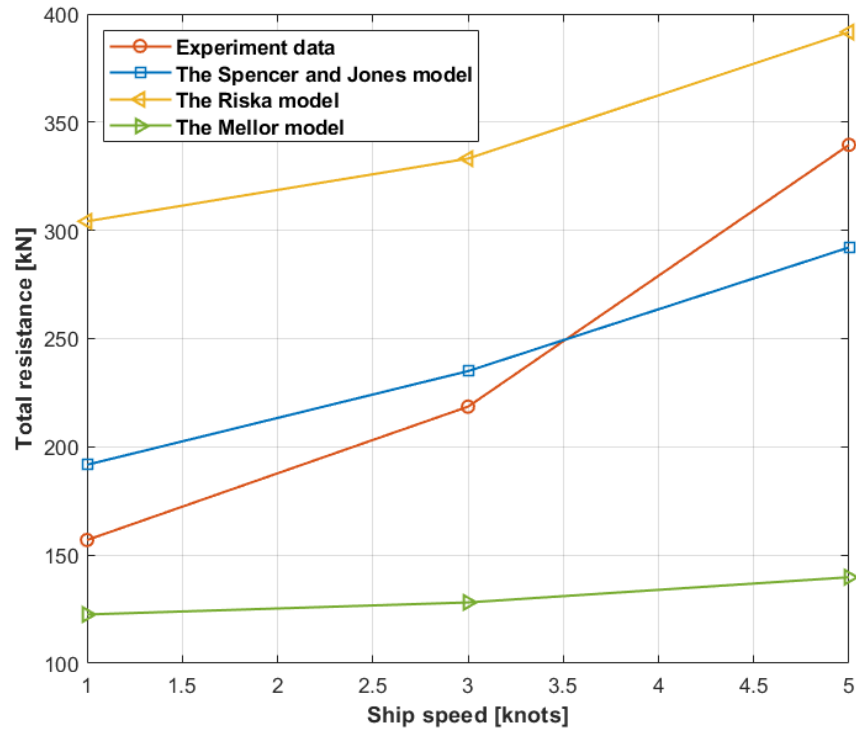


Figure 4.4: The comparison between model estimations with RV Araon model test in 0.86 m thickness brash ice condition.

Table 4.7: Brash ice resistance comparison between studied models and model tests.

Speed	1 knot	3 knots	5 knots	Average	Standard deviation
Error [%] - The Spencer and Jones model	22.14	7.51	-13.96	5.23	18.16
Error [%] - The Riska model	93.82	52.44	15.35	53.87	39.25
Error [%] - The Mellor model	-21.92	-41.38	-58.84	-40.71	18.47

From the comparison in figure 4.4 and table 4.7, the Spencer and Jones model performs better than the other two models, with the maximum error of 22% and an average error of only 5%. As the standard of classification, the Riska model is always on the conservative side of the results with the average overestimation of 54%. The Mellor model estimation also has large errors in this case with the average of 41% underestimation. This large error may be because the Mellor model as an entirely analytical model undervalues unknown influence and the suitable ship type is too conventional for the new designed ship.

4.4 Comparison for Case 3

Icebreaking tanker MT Uikku (now is known as Varzuga) is an Arctic product oil tanker operating in the Northern Sea Route and her principles are presented in table 4.8. Hu and Zhou (2016) designed a series of tests with her model (model scale = 1:31.56) in channel ice condition with the ice thickness of 0.63m and 1.04m respectively.

The model ice used in the tests was generated from ethanol solution and under strict growing temperature control to ensure its flexure strength. During the tests, the water density ρ_w and the ice density ρ_i were measured as 989 kg/m³ and 906 kg/m³ respectively, hence the same values are applied in the simulations. The ice-hull friction coefficient was determined as 0.04

via measurement. Other unknown variables are assumed the same as table 4.2 or average values used in Case 2.

Table 4.8: Principal particulars of the MT Uikku.

Length [m]	150
Length of bow [m]	39
parallel mid-body length [m]	65
Beam [m]	21.3
Draught [m]	9.5

Three brash ice resistance models are applied in the same condition as the model tests. Figure 4.5 and table 4.9 present the results of the comparison between tests and model predictions and these detailed values are attached in Appendix A.

Most of the estimates at ice thickness of 0.63 m are further from the model tests than at 1.04m. The Riska model is the safest one always on the conservative side and overestimates ice resistance 211% averagely. The results of the Spencer and Jones model are less conservative, and errors are in a quite wide range from 3% to 113%. However, the Mellor model estimates are always unsafe with the average of 46% undervalues.

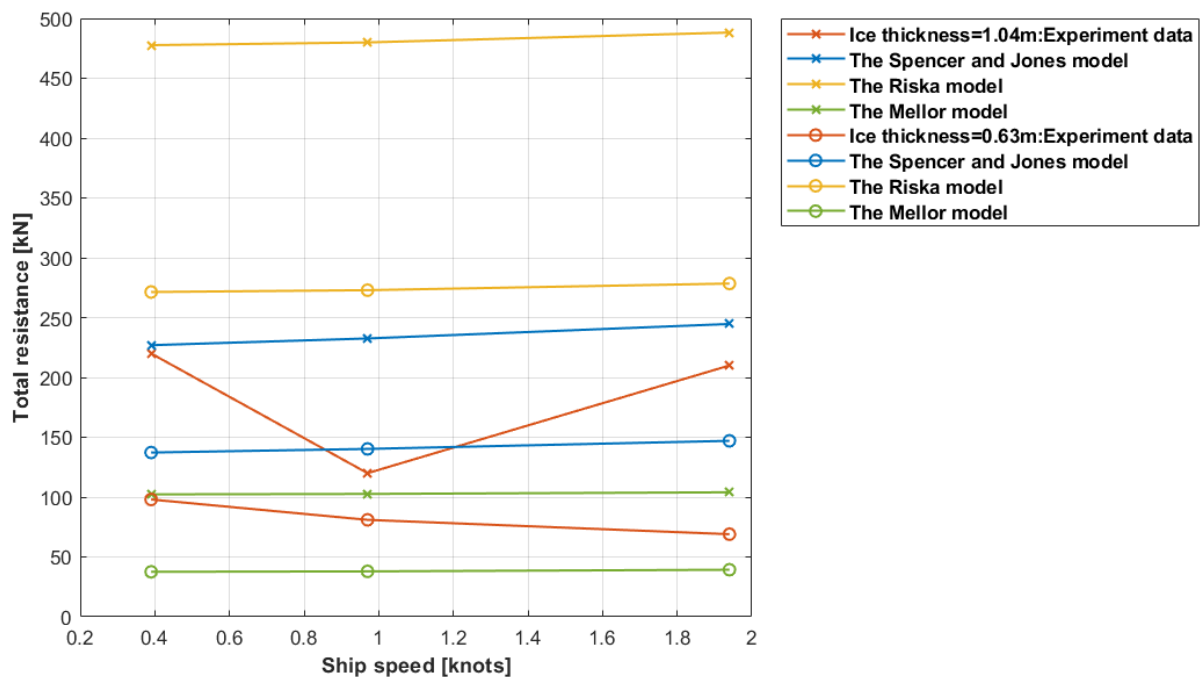


Figure 4.5: The comparison between model estimations with an icebreaking tanker model test in 1.04m and 0.63m thickness brash ice condition.

Table 4.9: Total ice resistance comparison between studied models and model tests in in 1.04m and 0.63m thickness brash ice condition.

Ice thickness	0.63 m			1.04 m			Average	Standard deviation
	0.39	0.97	1.94	0.39	0.97	1.94		
Error [%] - The Spencer and Jones model	40.05	73.16	113.08	3.16	93.81	16.51	56.63	43.79
Error [%] - The Riska model	176.93	236.93	303.55	117.12	299.95	132.48	211.16	81.60
Error [%] - The Mellor model	-61.66	-53.18	-43.06	-53.50	-14.46	-50.47	-46.05	16.59

4.5 Summary of case study

Broken ice models are compared for different ship types in Case 1 and Case 2. Both of them estimate poorly for ice resistance of the conventional Panamax with an average of more than 50% underestimation. Also, both predict better for the tankers in Case 1 than the icebreaker in Case 2. In Case 1, most estimates are within 50% errors while in Case 2 the inaccuracies are almost doubled. Two models have quite similar performances during the prediction above, it may be because both are based on the Colbourne theoretical analysis.

From the results presented in figure 4.6, it can be concluded that the Guo model, as a newer semi-empirical model, is slightly superior than the Woolgar and Colbourne model in most conditions. If the ice-hull friction coefficient could be defined in each case instead of using the average value, the Woolgar and Colbourne model might perform better.

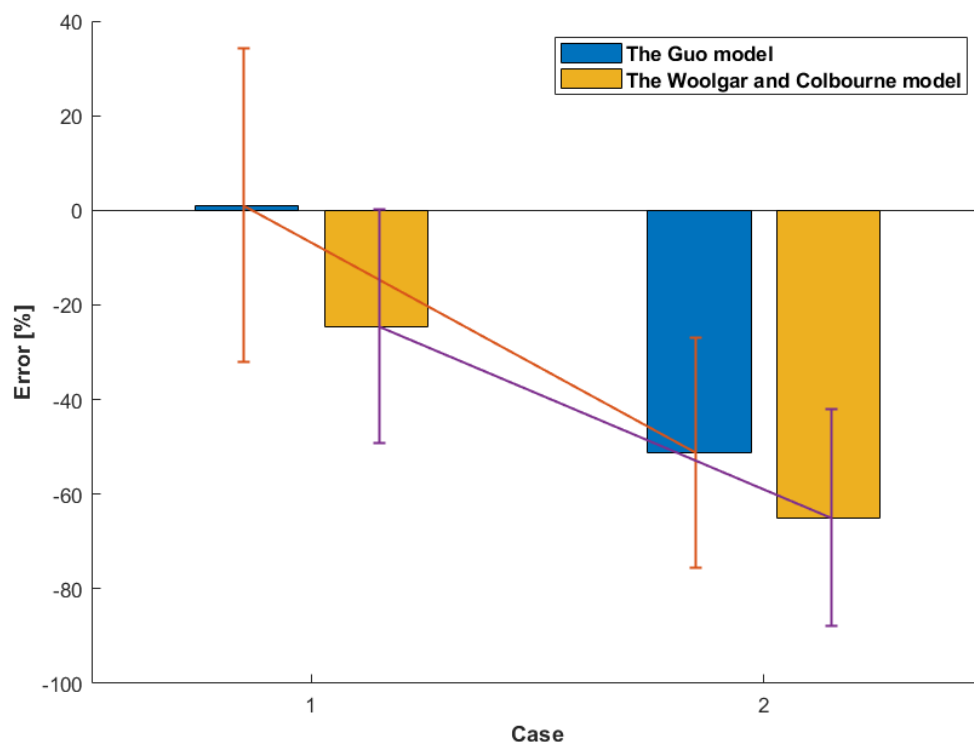


Figure 4.6: The summary of error distributions from different models in broken ice condition (Case 1 and Case 2).

As for brash ice models, three models predict quite differently with various discrepancies, deviating easily from 3% to 300%. The estimates from the Spencer and Jones model are the closest to the experimental results mostly. It predicts quite accurately for the icebreaker Araon with only 5% error averagely but much less fits with the tanker Uikku.

However, the Riska model poorly fits the measurements, well overpredicting all the time. This model was concluded from ten full-scale Baltic-classed merchant ships twenty years ago and the empirical variables might need to be updated for the newly designed ships to achieve better accuracy. Also, as a standard classification rule, the Riska model may take an unknown safety factor into consideration to predict ice resistance with enough safety margin.

At last, the Mellor model, as the only entirely analytical model, undervalues mostly with quite large errors as well. It might be for lack of geometry characteristics of the studied vessel, which is the key during a pure analytical method. Besides, the Mellor model only takes bow and parallel body resistance in ice into account and the uncertain factor is decided by the database in 40 years ago. Both need to be updated and modified to fit new designed ice-going ships nowadays.

Overall, even though the Spencer and Jones model is designed for R-class icebreakers, figure 4.7 indicates that its prediction results are still more applicable than the other two models for tankers in Case 3 and even better for icebreakers in Case 2 and it mostly tends to get a conservative prediction. To conclude, based on the discussion above, both broken ice models and the Spencer and Jones model are to be applied into ShipCLEAN tool for the ice resistance estimations.

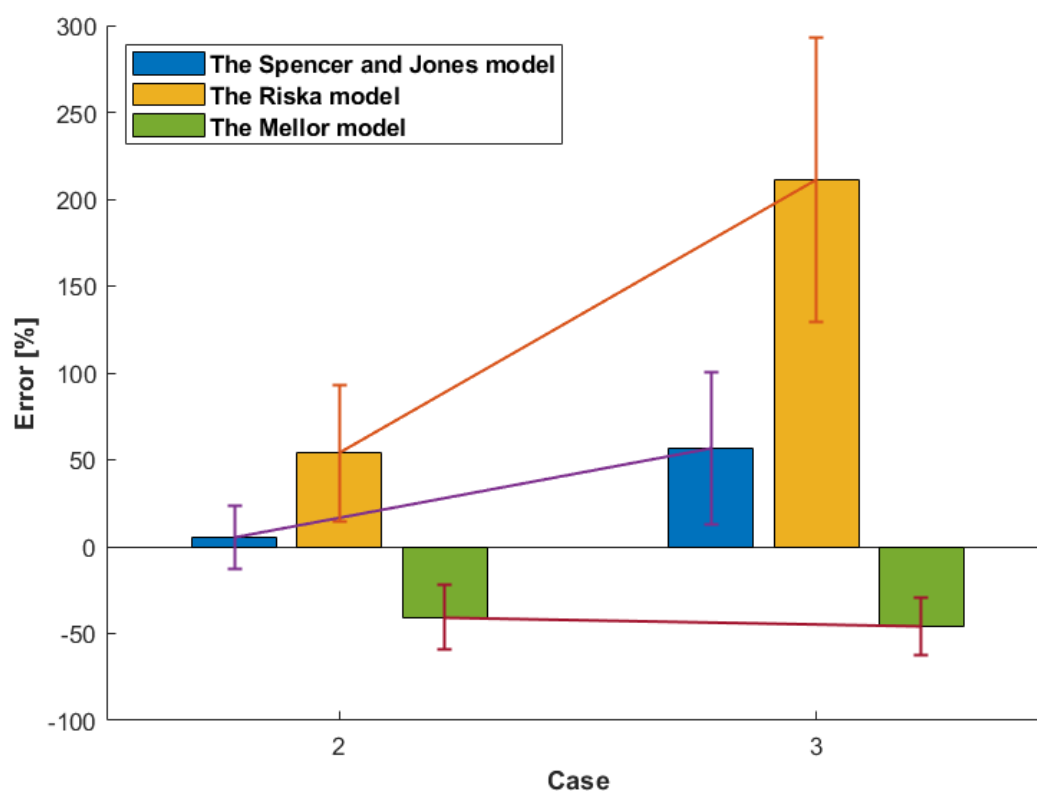


Figure 4.7: The summary of error distributions from different models in brash ice condition (Case 2 and Case 3).

5 Results and discussion

This chapter is to study the sensitivity of each parameter to ice resistance in different analytical methods and derive the fuel consumptions for certain conditions. The sensitivity study helps to understand that ice resistance is most sensitive with which parameter from ship hull or ice. A product tanker is studied in this chapter with its main principles shown in table 5.1. Total ship resistance and the required ship power are derived from ShipCLEAN tool by using the chosen ice resistance model. Also, the fuel consumptions of a selected route can be compared at various ice conditions.

Table 5.1: Characteristics of the product tanker.

Length overall [m]	183.0
Breadth [m]	32.2
Draft [m]	11.0
Design speed [knot]	15
Operational power [kW]	9727
Ice class	1A

5.1 Sensitivity analysis

Table 3.3 shows the different parameters that work as input in each analytical method. A sensitivity study of parameters, including ice density, ice thickness, concentration and ice-hull friction coefficient, is to be carried out in this section.

The sensitivity is shown in the ratio between change rate of ice resistance with the change rate of corresponding variable. Change rate of resistance and each variable are derived by,

$$Resistance\ change\ rate = \frac{Ice\ resistance\ after\ change - original\ ice\ resistance}{original\ ice\ resistance} \times 100\% \quad (5.1)$$

$$Parameter\ change\ rate = \frac{changed\ value - reference\ value}{reference\ value} \times 100\% \quad (5.2)$$

It needs to be noted that one parameter's sensitivity may change with another input. Hence three different ship (3 knots, 5 knots and 7 knots) speed is applied here to show the influence of speed to each parameter's sensitivity. Only a part of the results is shown in the following text, as for more additional graphs are attached in the Appendix B.

Based on the Arctic summer state, the reference parameters are listed here:

Table 5.2: Reference input parameters.

Ice density [kg/m ³]	900
Ice thickness [m]	1.0
Concentration [-]	60%
Ice-hull friction coefficient [-]	0.13

The ice-hull friction coefficient of 0.13 is the average value suggested by Woolgar and Colbourne (2010).

5.1.1 Ice density

Ice density is an important factor in all the analytical methods. However, its values vary over a quite wide range from 720 kg/m³ to 940 kg/m³ in the Arctic area (Timco & Weeks, 2010).

The longer the sea ice sheet age, the smaller the density due to the exudation of the marinade in the ice. Hence, the sea ice density is less in summer than in the winter.

Here all the possible values of ice density are set for the sensitivity study. Figure 5.1 shows the sensitivities of ice density from different models with the ice density range from 720 kg/m³ to 940 kg/m³. Also, since this thesis focuses more on the summer condition, the results at 10% reduction of ice density at different speeds are summarized in figure 5.2.

The ice resistance of two broken ice models presents the same linear relationship with the change of ice density, while three brash ice models tend to increase the resistance with the reduction of ice density. Especially, the Spencer and Jones model and the Mellor model rise almost half of the ice resistance. In contrast, the Riska model grows at a slower rate (about 10%).

Two ice types perform opposite trends when ice density changes, which is because of their difference of ice concentration. When a ship sailing at a low ice concentration, the ice floes around have enough space to move away from the trail; however, at higher ice concentration, these ice floes are crowdedly distributed over the sea and they are more likely to be submerged under the hull than to be pushed away. These two forces form from each ice floe's weight and the density difference between ice and sea water respectively, which are opposite in trend.

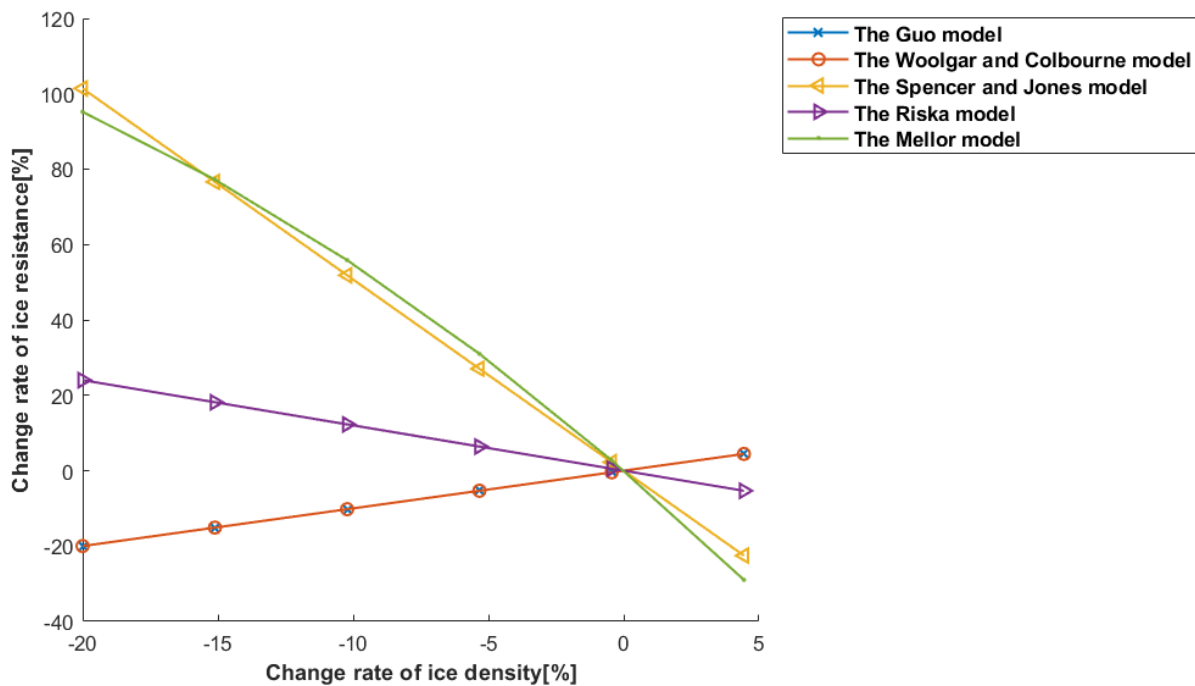


Figure 5.1: Sensitivities of ice density. (ship speed = 5 knots).

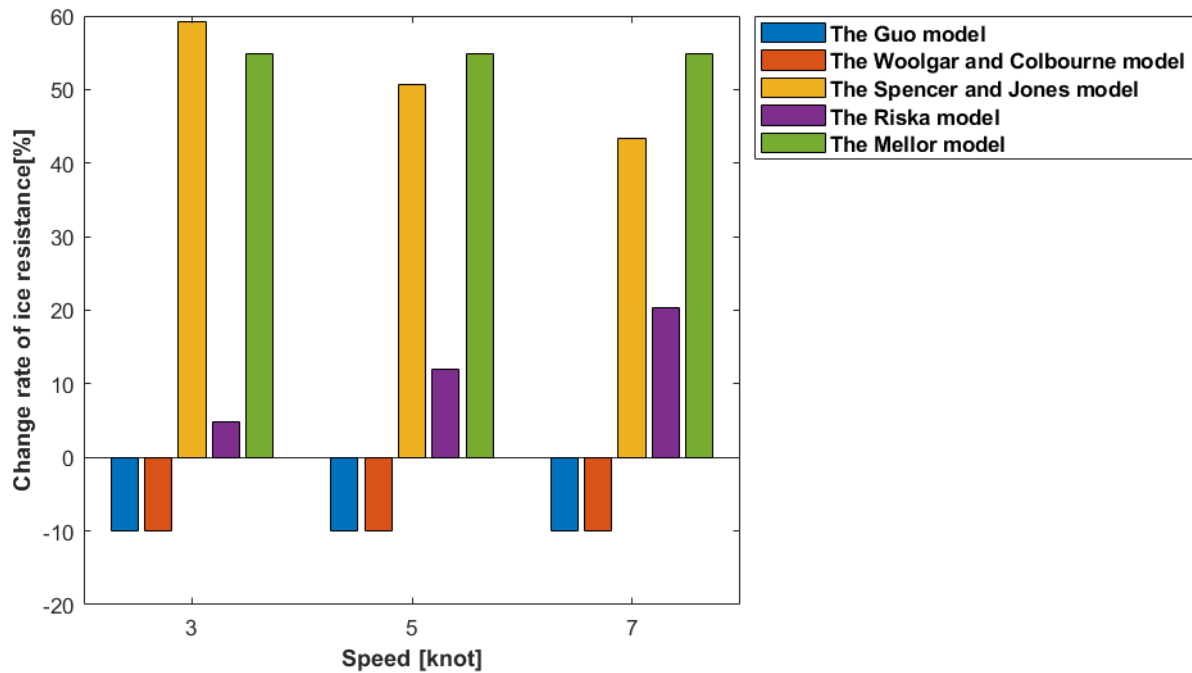


Figure 5.2: Sum of sensitivities of ice density.

5.1.2 Ice thickness

Ice thickness is an essential parameter in all the analytical methods, as it influences the volume and weight of ice floes and ice force on the offshore structure is a direct function of it. In MIZ, ice sheet is mostly within 2.5 m thickness (Weeks & Hibler, 2010). Here a range of $\pm 50\%$ of 1 m ice thickness is set for the sensitivity study.

Figure 5.3 clearly presents that the ice resistance estimates from all the models increase with ice thickness. However, each model shows a different growing trend as the ice thickness increased.

Besides, figure 5.4 sums up the sensitivities of ice thickness for all the models and all the speeds at 50% growth and this growth is slightly influenced by the ship speed. The Mellor model is the most sensitive with ice thickness, growing more than 120% in this situation, while another two brush ice models only with half of its growth rate, while the Riska model and the Spencer and Jones model are the least sensitive with ice thickness only raise around 55%.

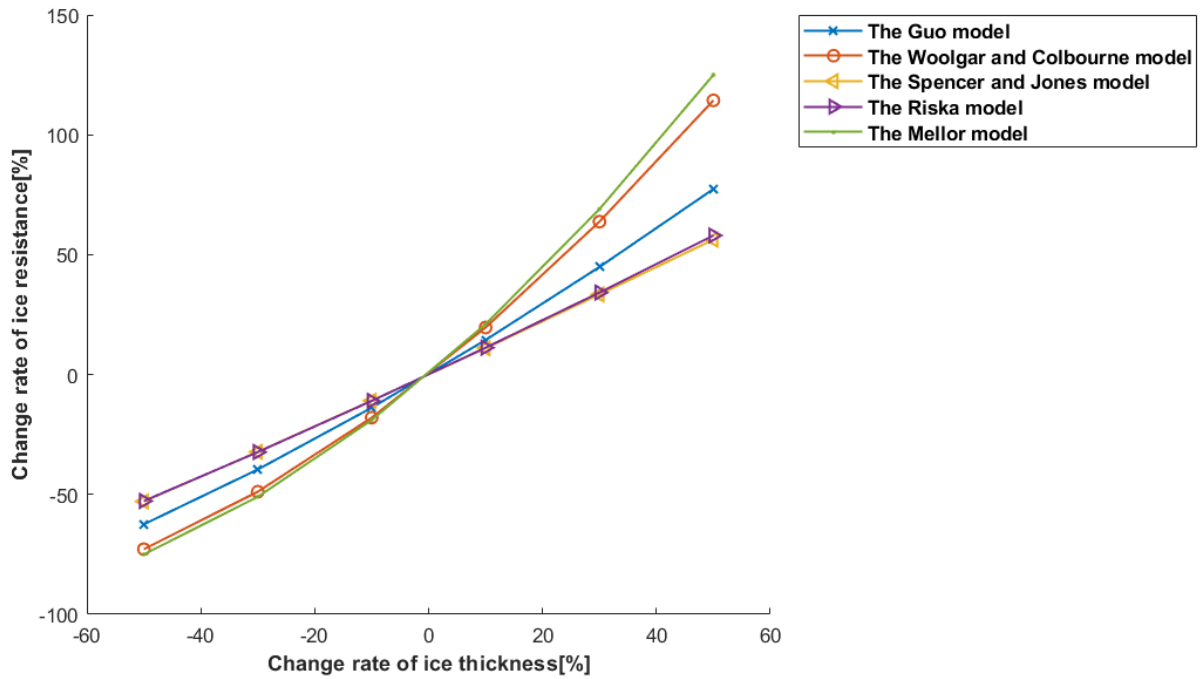


Figure 5.3: Sensitivities of ice thickness. (ship speed = 5 knots).

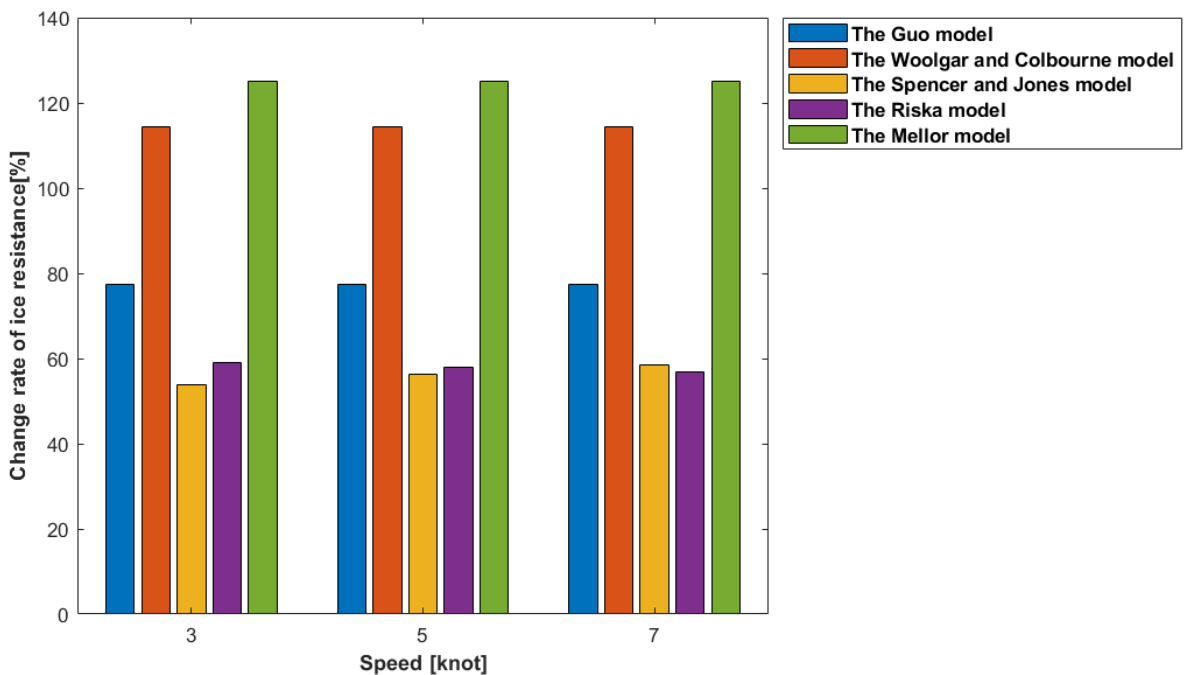


Figure 5.4: Sum of sensitivities of ice thickness.

5.1.3 Ice concentration

Since ice concentration is a factor that only appears in broken ice condition, two broken ice models are compared in a range from 0.4 to 0.7 of ice concentration. Also, from equations 3.1 to 3.9, it can be found that ice concentration is an independent factor on ship speed. The prediction results from both models are shown in figure 5.5.

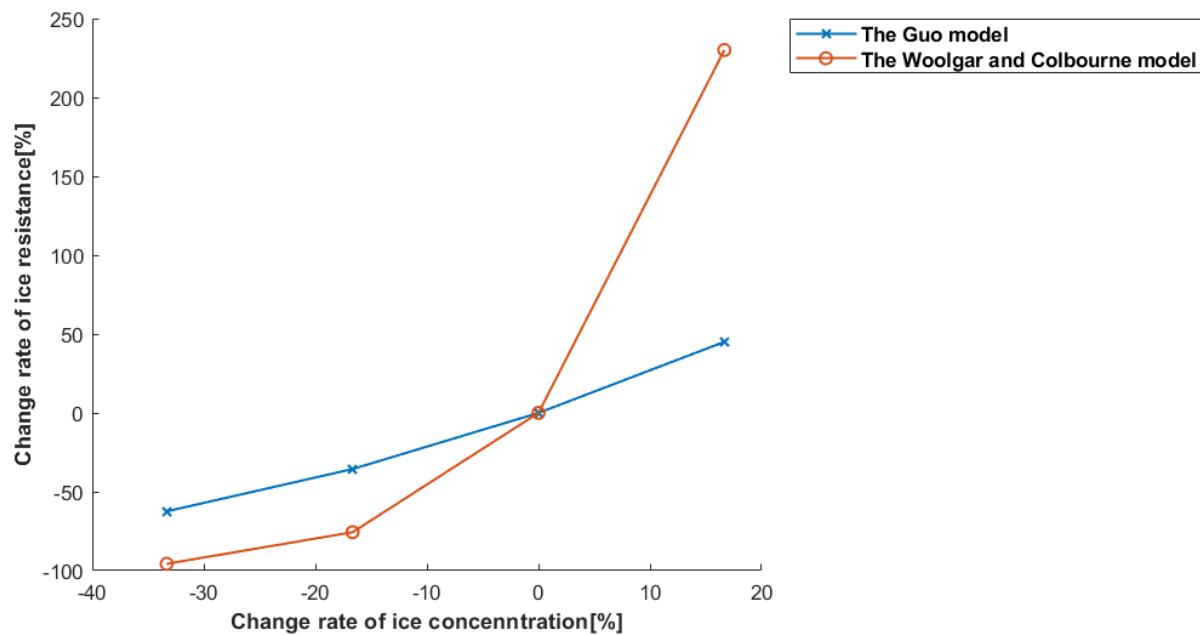


Figure 5.5: Sum of sensitivities of ice concentration.

Two models display quite different ice concentration sensitivities and it is clear in figure 5.5 that the Woolgar and Colbourne model is quite sensitive. The ice resistance from the Guo model grows around 30% at while the Woolgar and Colbourne model more than double the ice resistance when ice concentration increases from 0.6 to 0.7.

In the Woolgar and Colbourne model, they decided to make pack ice coefficient related to ice concentration and from their results, it can be found they believed ice resistance is very sensitive to ice concentration.

5.1.4 Ice-hull friction coefficient

During sailing, broken ice floes slide along ship hull, which lead to a friction force is a function with ice weight and also hull condition. If the ship is old and badly corroded, the ice-hull friction will be larger than a newly built ship. In order to describe the ice-hull friction condition in different scales, ice-hull friction coefficient was defined as the ratio between friction resistance force and ice weight (Hu & Zhou, 2016).

Since only the Woolgar and Colbourne model has ice-hull friction coefficient parameter, it is the only method used for its sensitivity study. Ice-hull friction coefficient has a quite wide range from 0.01 to 0.5 (Lau, 2018) and it is dependent on the material, painting condition, corrosion and so on.

A wide range of ice-hull friction coefficient from 0.03 to 0.43 is applied in its sensitivity study, and the results are shown in figure 5.6. Ice resistance increases around 25% when ice-hull friction coefficient is doubled to 0.26, and this parameter is independent on ship speed in this model.

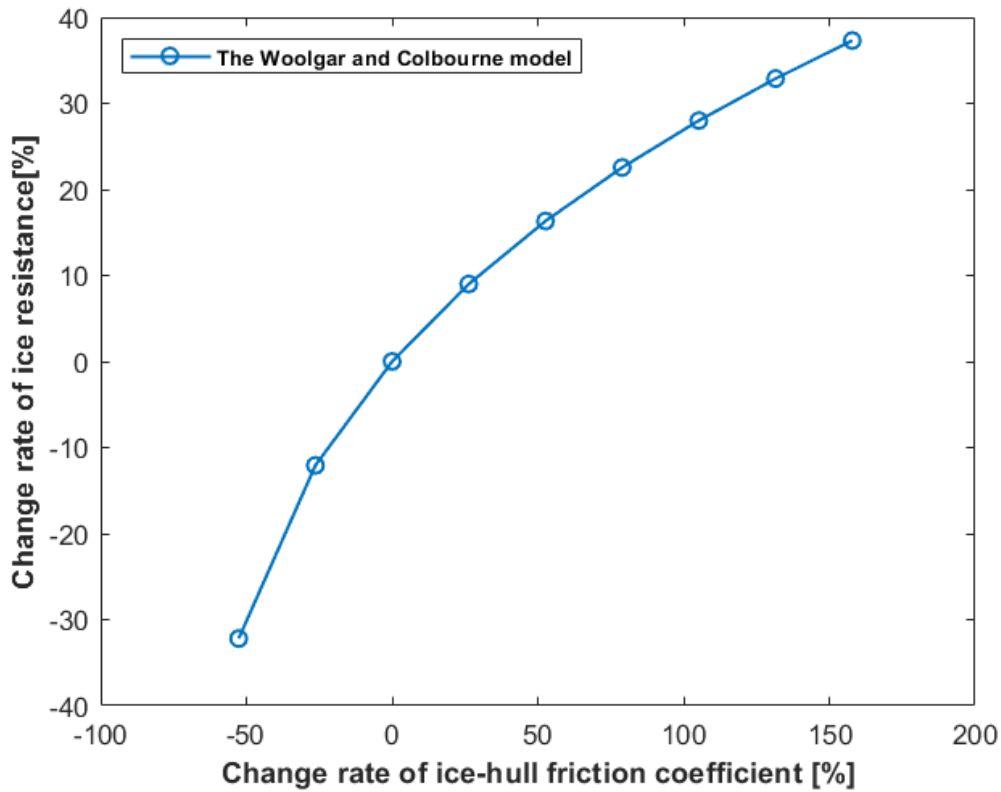


Figure 5.6: Sensitivity of ice-hull friction coefficient.

5.1.5 Results and discussion of sensitivity study

Here a brief summary of all the results in the sensitivity study is shown in table 5.3. From the sensitivity analysis, it is clear that the ice thickness and ice concentration are the main factors influencing ice resistance in all the studied models. Besides, from the Woolgar and Colbourne model, ice-hull friction is also a key influence needs to be taken into consideration.

Table 5.3: Summary of sensitivity analysis.

Parameter	Reference value	Range	Changed Value	Resistance change rate
Ice density [kg/m^3]	900	720-940	810	-20%~100%
Ice thickness [m]	1.0	0-2.0	1.5	56%~125%
Ice concentration [-]	0.6	0-1.0	0.7	45%~230%
Ice-hull friction coefficient [-]	0.13	0.03-0.50	0.43	37%

5.2 Ice resistance module of the ShipCLEAN model

After the comparison in chapter 4, it is concluded that the Spencer and Jones model are more applicable with limited ship data for the ice resistance prediction in brash ice condition. Their results are with less errors in case study, hence they are more reliable to be used for the ice resistance prediction.

As for broken ice resistance simulations, these two models are quite similar and both of them are applied into ShipCLEAN to implement the tool for the further calculations of total resistance, required power and fuel consumption.

Since brash ice condition is the route left by icebreakers, it is the accumulated wreckage of broken level ice and with nearly 100% concentration. When ice concentration is more than

95% in the application, this ice condition is closer to brash ice. Brash ice resistance is lower than the broken ice resistance at rather high ship speed and concentration, that is it would be easier for commercial ship to run with the assistance of an icebreaker than to navigate alone in higher concentration pack ice. Hence, in the ice resistance module of the ShipCLEAN model, it is assumed that ice concentration less than 95% is in broken ice condition and others is in brash ice condition.

It should be noted that in some severe ice conditions if the ship resistance is too large to stay at the target speed, the studied ship will have to sacrifice a part of the speed to keep running.

5.3 Ship route

In this section, a part of the Northern Sea route is set from the Port of Petropavlovsk – Kamchatskiy to the Port of Murmansk, shown in figure 5.7. The length of the whole route is estimated 9,048 kilometres (around 4886 nautical miles). The latitude and longitude coordinates in this route are collected and applied into ShipCLEAN tool to simulate the voyage and estimate the fuel consumption.

With limited information of this route, some assumptions are made for the sea states: wave height is 1 meter without direction; water depth is 50 m; no wind or current speed. Besides, the tanker is simulated to operate in two operation conditions: one is to keep sailing with full load by the fixed sailing time of 520 hours (that is the minimum sailing time the studied ship could achieve in November), and another is to keep sailing with full load by a longer fixed time of 750 hours.

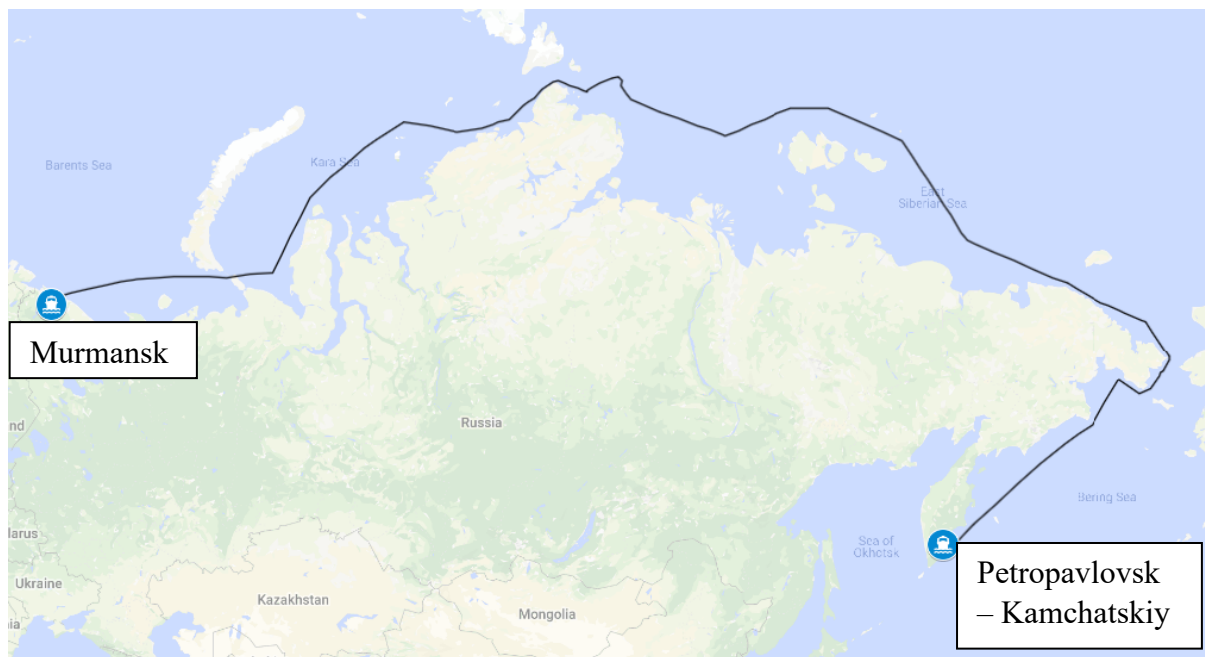


Figure 5.7: The selected route in the ShipCLEAN.

In the Arctic region, the summertime lasts from the end of June to September every year and the ice sheet keeps melting. There is nearly no ice in the edge of the Arctic sea during September. The weather records of July, October and November in 2018 are collected and shown in figure 5.8.

Based on the previous setting, the sailing time and fuel consumption estimations in open-water condition and various ice conditions are studied and computed by ShipCLEAN tool and compared in table 5.4. The increasements of total fuel consumption of these months compared to open-water condition are compared in figures 5.8 and 5.9.

Two different broken ice resistance models give quite different predictions, the Woolgar and Colbourne model always underestimate the resistance than the Guo model. In the most severe condition, their fuel consumption estimate difference can reach a maximum of around 150t.

From the results, it can be found that the ice impact on the fuel consumption is quite large, in the most severe ice condition (November) the fuel consumption is almost 180% of the same route without ice. If the studied ship increases its target sailing time from 520 hours to 750 hours, that is to lower speed, the fuel consumption can lower to one half in the Guo model prediction.

Figures 5.11 to 5.13 show the estimations of ship speed, required power and fuel consumption rate in the fixed journey time of 520 hours without ice and with ice in November respectively. Further results for other situations are attached in Appendix C. In the ship speed part, the speed change violently under this severe ice condition.

In quite severe ice condition like from the route 1700nm to 2100nm in November, the engine keeps working in a quite low propulsion power and fuel consumption rate. That is because the ice resistance increases the total resistance significantly and when the thrust is constant, the ship speed will decrease accordingly; the reduction of the ship speed will reduce the advance ratio of the propeller and the diesel engine speed. The speed will drop and the power generated will be reduced. At the end, the ship will reduce the propulsion and the ship's resistance (the air resistance and water resistance of the ship will be greatly reduced when the speed of the ship is reduced).

In addition, in the mildest ice condition (October), the ship can almost navigate normally by the same speed as it does without ice. From the predicted results, fuel consumption is the same in the Woolgar and Colbourne model and only 1 ton more than without ice in the Guo model. Also, it's clear in Appendix C that the speed doesn't change in this mild ice condition at all.

Table 5.4: Sailing time and total fuel consumption estimations.

		Open water	July	October	November
		No ice	With ice	With ice	With ice
Time [hour]		520	520	520	520
Fuel consumption [t]	The Guo model	187.5	307.4	188.4	533.9
	The Woolgar and Colbourne model	187.5	235	187.5	379.5
Time [hour]		750	750	750	750
Fuel consumption [t]	The Guo model	126.3	209.2	127.1	255.7
	The Woolgar and Colbourne model	126.3	157.6	126.4	219.1

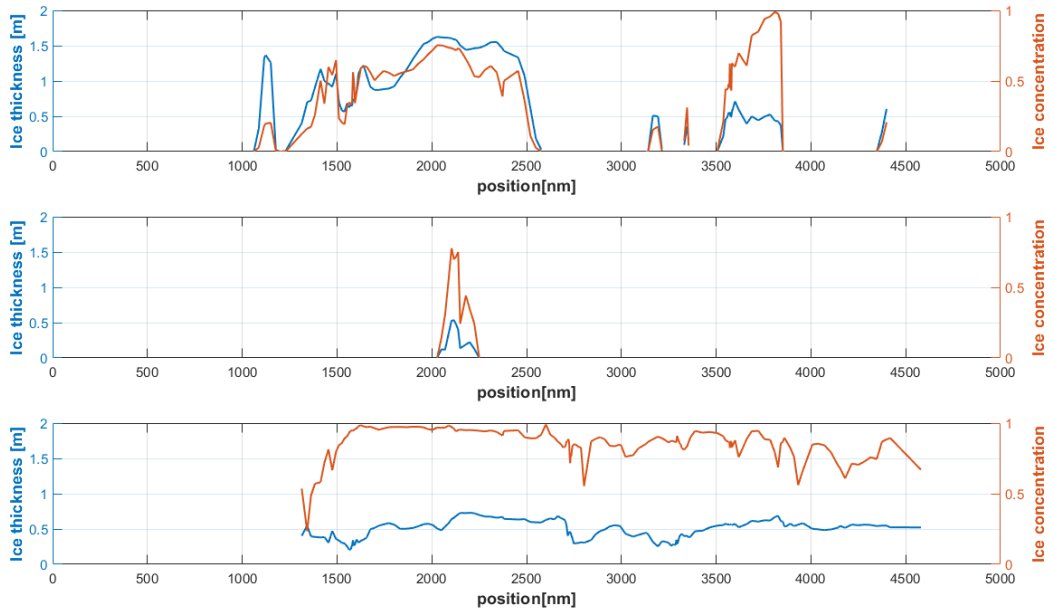


Figure 5.8: Ice conditions of the selected route in July (top), October (middle) and November (bottom) 2018.

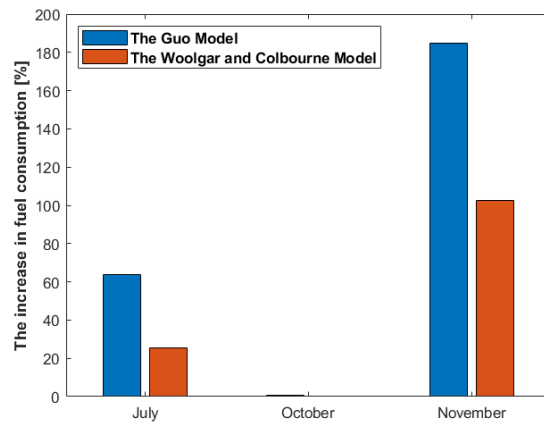


Figure 5.9: The increases of total fuel consumption estimates at each month with fixed journey time of 520 hours.

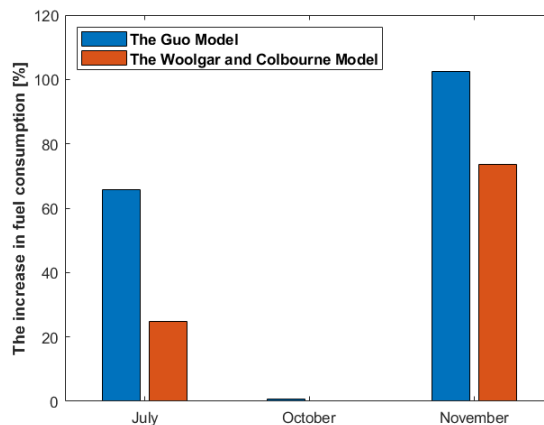


Figure 5.10: The increases of total fuel consumption estimates at each month with fixed journey time of 750 hours.

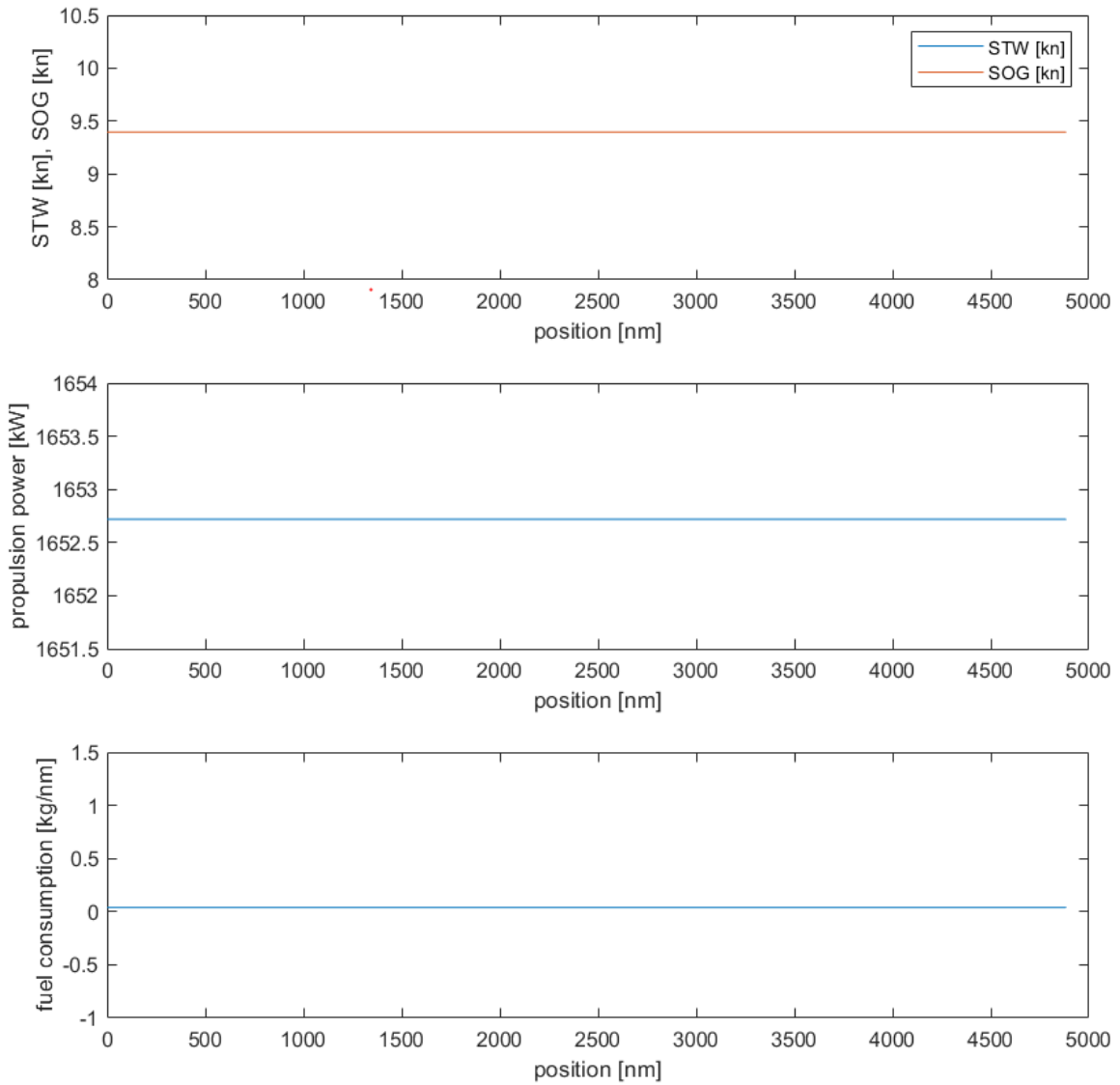


Figure 5.11: Ship speed, fuel consumption rate and propulsion power estimations with fixed journey time of 520 hours without ice.

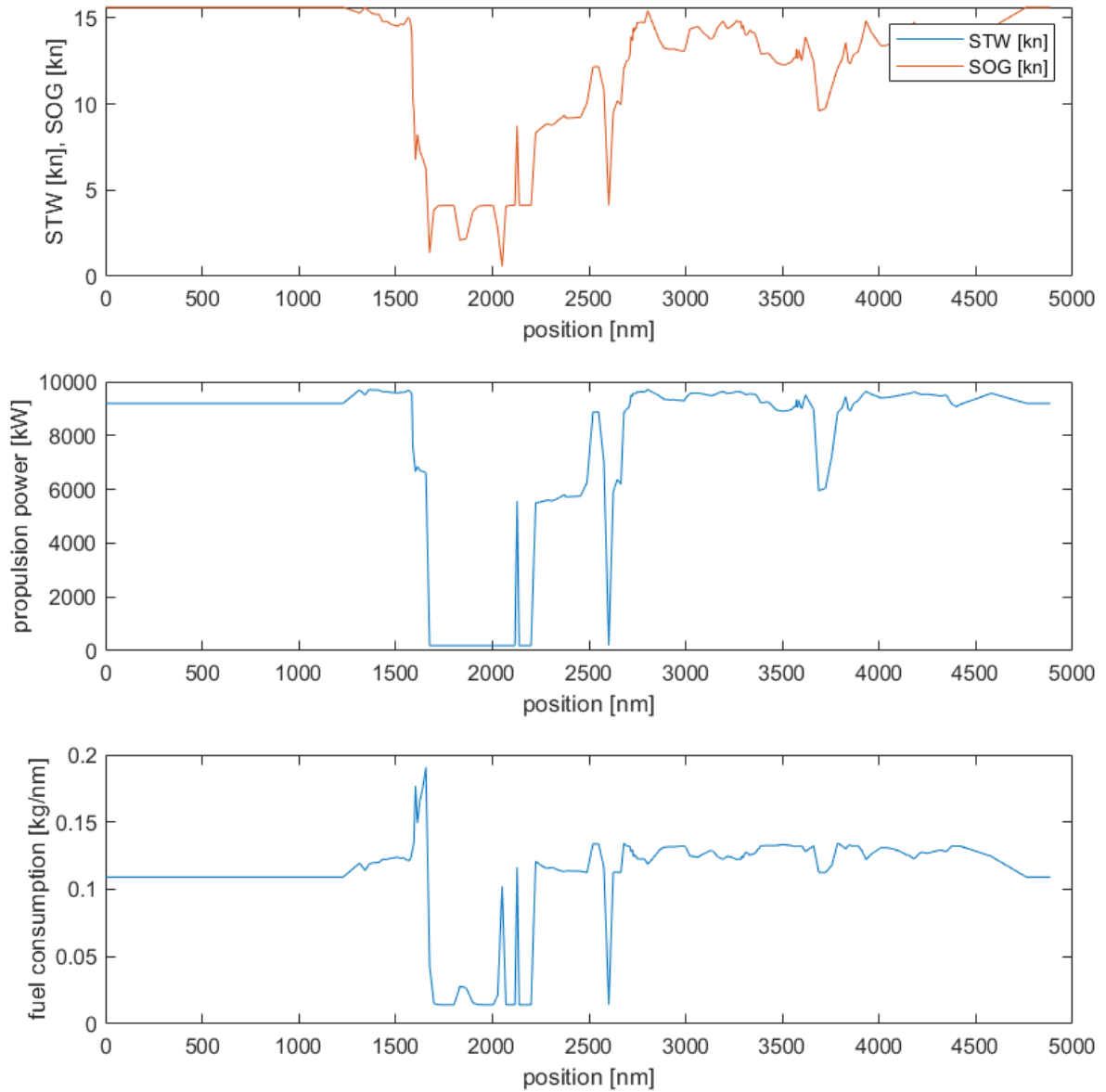


Figure 5.12: Ship speed, fuel consumption rate and propulsion power estimations with fixed journey time of 520 hours in 2018 November ice conditions. (The Guo model).

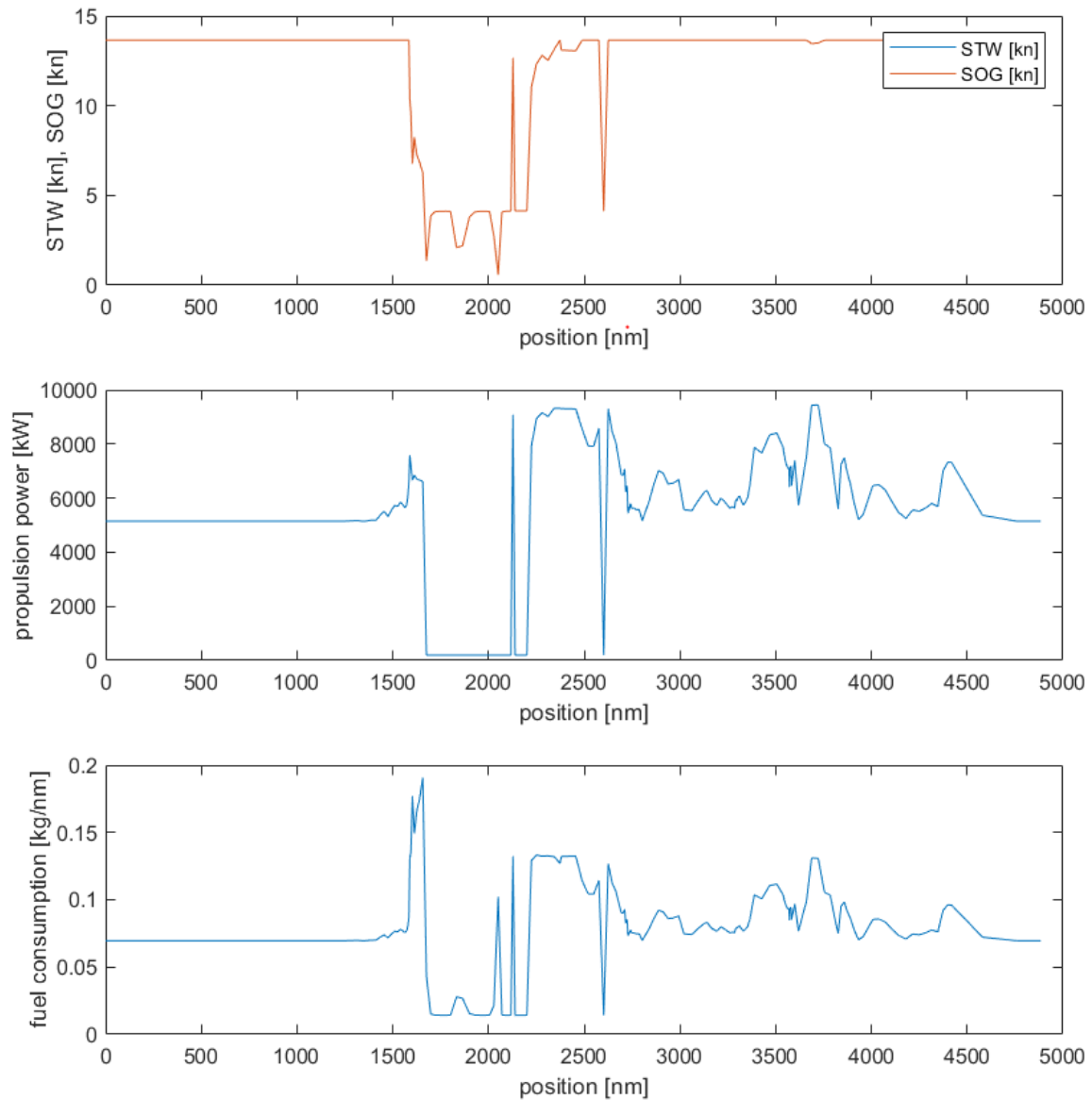


Figure 5.13: Ship speed, fuel consumption rate and propulsion power estimations with fixed journey time of 520 hours in 2018 November ice conditions. (The Woolgar and Colbourne model).

6 Summary and conclusions

From the comparison case study, different semiempirical formulae predict quite different ice resistance and it is clear to find ship shape has the most impact on ice resistance, since the errors among cases vary a lot. When the studied ship type is close to the semiempirical model, the prediction is rather accurate, and the prediction error is limited within 40% mostly.

The entirely analytical method, the Mellor model is less affected by the ship shape compared to others. However, it may not take enough effects into consideration and always underestimates ice resistance, which is pretty unsafe for the engineering use. Also, it is a pure physical analysis built 40 years ago. With the development of ship shapes in these years, it also needs to be modified and updated for the new ships.

Under the simplified conditions in these studied cases, it can be concluded that the Guo model and the Spencer and Jones model are recommended to be used for the prediction of ice resistance with limited information from both ice and ship hull. Nevertheless, the estimates' errors from two broken ice models are quite close, if the ice-hull friction coefficient could be known, the Woolgar and Colbourne model might perform better.

From the sensitivity analysis, it is clear that the ice thickness and ice concentration are the main factors influencing ice resistance in all the studied models. Besides, from the Woolgar and Colbourne model, ice-hull friction is also a key influence needs to be taken into consideration.

It is found from the estimated results that fuel consumption is more influenced by the presence of sea ice at higher speed, because the increase of fuel consumption is more than 100-180% at 10 knots target speed while 70-100% at designed speed in the relatively severe ice condition of November.

Finally, it can be concluded that sea ice has a significant impact on ship resistance, even when ice-going ships sailing in crushed ice floes. At the same sailing time, the ship is more affected by ice resistance at high speeds in cost of fuel. However, this is concluded at almost calm sea condition, nearly no wave or current speed is considered and also the coupling resistance between wave and ice is ignored in this thesis.

7 Future work

The objective is to review and compare ice resistance models regarding the Arctic marginal ice zone and apply the chosen ones into ShipCLEAN tool to predict fuel consumption in different weather conditions. Some limitations in this thesis study could be further developed in future work.

To have a clearer comparison between case and model estimations, discrete element method could be applied to compare the estimated results with FE models and some simplifications in resistance calculation can be avoided.

The ice density is also a necessary input in most models for ice resistance prediction and it is assumed to be stable in this thesis. The relationship between ice density and environment temperature, ice thickness could be investigated and defined into a function to achieve a more accurate simulation.

In Section 5.3, the route is analysed in calm water and the water depth is assumed to be the same all along the route. More accurate sea state could be found and added into comparison part. Also, it could also be useful to investigate the coupling force caused by wave–ice floe–ship interaction in marginal ice zone.

8 References

- Aboulazm, A. & Muggeridge, D., 1990. *Ship model testing in simulated ice floe covered waters..* St. John's, Newfoundland, Canada, American towing tank conference.
- Colbourne, D. B., 2000. Scaling Pack Ice and Iceberg Loads on Moored Ship Shapes. *Oceanic Engineering International*, 4(1), pp. 39-45.
- Colbourne, D. B. & Lever, J. H., 1992. Development of a Component-Based Scaling System for Ship-Ice Model Test. *Journal of Ship Research*, 36(1), pp. 77-87.
- Corlett, E. & Snaith, G., 1964. Some aspects of icebreaker design. *The Royal Institution of Naval Architects*, 106(4), pp. 389-413.
- Cox, G. & Weeks, W., 1983. Equations for determining the gas and brine volumes in sea ice samples. *Journal of Glaciology*, 29(102), pp. 306-316.
- Eguíluz, V. M., Fernández-Gracia, J., Irigoien, X. & Duarte, C. M., 2016. A quantitative assessment of Arctic shipping in 2010–2014. *Scientific Reports*, Volume 6.
- Enkvist, E., 1972. *On the ice resistance encountered by ships operating in the continuous mode of icebreaking*, Finland: Swedish Academy of Engineering Sciences.
- Enkvist, E., 1983. *A survey of experimental indications of the relation*. Helsinki, Finland, 7th International Conference on Port and Ocean Engineering under Arctic Conditions (POAC 83), pp. 484-493.
- Evers, K.-U. & Jochmann, P., 1993. *An Advanced Technique to Improve the Mechanical Properties of Model Ice*. s.l., POAC'01.
- Gao, Y., Hu, Z., Ringsberg, J. W. & Wang, J., 2015. An elastic–plastic ice material model for ship-iceberg collision simulations. *Ocean Engineering*, Volume 102, pp. 27-39.
- Guo, C.-y.et al., 2018. Experimental Investigation of the Resistance Performance and Heave and Pitch Motions of Ice-Going Container Ship Under Pack Ice Conditions. *China Ocean Engineering*, 32(2), pp. 169-178.
- Harder, S., 2009. *Arctic marine shipping assessment*, s.l.: Arctic Council.
- Hu, J. & Zhou, L., 2016. Further study on level ice resistance and channel resistance for an icebreaking vessel. *International Journal of Naval Architecture and Ocean Engineering*, 8(2), pp. 169-176.
- Ionov, B., 1988. *Ice Resistance and its Composition [in Russian]*, Gidrometeoiztat, Lenigrad: Arctic and Antarctic Research Institute.
- ISO/FDIS/19906, 2010. *Petroleum and natural gas industries-Arctic offshore structures..* Geneva, Swizerland, International Standard. International Standardization organization..
- ITTC, 2011. *Fresh Water and Seawater Properties*. s.l., International Towing Tank Conference 7.5-02-01-03.

- Jones, S., 1989. *A Review of Ship Performance in Level Ice*. The Hague, Netherlands, Proceedings of the 8th International Conference on Offshore Mechanics and Arctic Engineering, pp. 325-342.
- Juva, M. & Riska, K., 2002. *ON THE POWER REQUIREMENT IN THE FINNISH-SWEDISH ICE*, Espoo: HELSINKI UNIVERSITY OF TECHNOLOGY.
- Kim, H.-S., Lee, C.-J., Choi, K.-S. & Kim, M.-C., 2011. Study on icebreaking performance of the Korea icebreaker ARAON in the arctic sea. *International Journal of Naval Architecture and Ocean Engineering*, 3(3), pp. 208-215.
- Kim, H. S., Han, D., Go, B. & Jeong, S.-Y., 2018. *Prediction of Attainable Ship Speed in Brash Ice Using Empirical Formula*. Sapporo, Japan, s.n.
- Kitazawa, T. & Ettema, R., 1985. Resistance to ship-hull motion through brash ice. *Cold Regions Science and Technology*, pp. 219-234.
- Kovas, A., 1996. *Bulk salinity versus ice floe thickness*, Hanover, NH, U.S.A.: CRREL.
- Kulyakhtin, S. & Høyland, K. V., 2015. Ice rubble frictional resistance by critical state theories. *Cold Regions Science and Technology*, Volume 119, pp. 145-150.
- Lau, M., 2018. Friction correction for model ship resistance and propulsion tests in ice at NRC's OCRE-RC. *International Journal of Naval Architecture and Ocean Engineering*, Volume 10, pp. 413-420.
- Lau, M., Wang, J. & Lee, C., 2007. *Review of ice modeling methodology*. Dalian, China, Recent Development of Offshore Engineering in Cold Regions.
- Levine, G., Voelker, R. & Mentz, P., 1974. Advances in the Development of Commercial Ice-Transiting Ships. *SNAME Transactions*, Volume 82, pp. 313-343.
- Lewis, J. W. & Edwards, R. Y., 1970. *Methods for predicting icebreaking and ice resistance characteristics of icebreakers*. s.l., SNAME.
- Lindqvist, G., 1989. *A Straightforward Method For Calculation of Ice Resistance of Ships*. Lulea, Sweden, Lulea University of Technology, Department of Civil Engineering, pp. 772-735.
- Li, Z. et al., 2000. Physical Behavior and Elastic Modulus of DUT-1 Ice. *Progress in Natural Science*, 10(10), pp. 931-935.
- Luo, W., Guo, C., Wu, T. & Su, Y., 2018. Experimental research on resistance and motion attitude variation of ship-wave-ice interaction in marginal ice zones. *Marine Structures*, pp. 399-415.
- Mäkinen, E., Liukkonen, S., Nortala-Hoikanen, A. & Harjula, A., 1994. *Friction and hull coatings in ice operations*. Calgary, Alberta, Canada, 5th International Conference on Ships and Marine Structures in Cold Regions.
- Mellor, M., 1980. Ship Resistance in Thick Brash Ice. *Cold Regions Science and Technology*, Volume 3, pp. 305-321.

- Mikko Juva, K. R., 2002. *ON THE POWER REQUIREMENT IN THE FINNISH-SWEDISH ICE*, Espoo: Helsinki University of Technology.
- Molyneux, W. D. & Kim, H. S., 2007. *Model experiments to support the design of large icebreaking tankers*. London, UK, Design and Construction of Vessels Operating in Low Temperature Environments.
- Myland, D. & Ehlers, S., 2018. *Investigation on semi-empirical coefficients and exponents of a resistance prediction method for ships sailing ahead in level ice*. Gothenburg, Sweden, s.n.
- Paavilainen, J., Tuhkuri, J. & Polojärvi, A., 2011. 2D numerical simulations of ice rubble formation process against an inclined structure. *Cold Regions Science and Technology*, Volume 68, pp. 20-34.
- Pernas Sánchez, J. et al., 2012. Numerical modeling of ice behavior under high velocity impacts. *International Journal of Solids and Structures*, 49(14), pp. 1919-1927.
- Riska, K., Wihelmsen, M., Kim, E. & Leiviska, K., 1997. *Performance of Merchant Vessels in Ice in the Baltic*, Espoo: Helsinki University of Technology.
- Schulson, E. M., 2001. Brittle failure of ice. *Engineering Fracture Mechanics*, Volume 68, pp. 1839-1887.
- SNAME, 1988. *Vol.2 Resistance Propulsion and Vibration*. New Jersey, s.n., pp. 57-62.
- Spencer, D. & Jones, S. J., 2001. Model-Scale/Full-Scale Correlation in Open Water and Ice for Canadian Coast Guard “R-Class” Icebreakers. *Journal of Ship Research*, 45(4), p. 249–261.
- Spencer, D. & Timco, G. W., 1990. *CD Model Ice - a process to produce correct density(CD) model ice*. Espoo, Finland, 10th International Symposium on Ice.
- Su, B., Riska, K. & Moan, T., 2010. A numerical method for the prediction of ship performance in level ice. *Cold Regions Science and Technology*, pp. 177-188.
- Sun, Q., 2005. *Research on the Mechanical Behavior of Ice and Interaction Force Problem of Ice with Sea Structure*. PHD Dissertation, Harbin, China: Harbin Engineering University.
- Tan, X., Su, B., Riska, K. & M. T., 2013. A six-degrees-of-freedom numerical model for level ice–ship interaction. *Cold Regions Science and Technology*, August, Volume 92, pp. 1-16.
- Tasnim News Agency, 2019. *Antarctic Sea Ice Collapse Rises Potential of 10-Foot Sea Level Rise: Study*. [Online] Available at: <https://www.tasnimnews.com/en/news/2019/01/16/1924589/antarctic-sea-ice-collapse-rises-potential-of-10-foot-sea-level-rise-study> [Accessed 16 January 2019].
- The MathWorks Inc, 2010. *MATLAB Version 9.5.0.944444 (R2018b)*, Natick, MA, United States.
- Timco, G., 1986. EG/AD/S: A new type of model ice for refrigerated towing tanks. *Cold Regions Science and Technology*, 12(2), pp. 175-195.
- Timco, G. & Weeks, W., 2010. A review of the engineering properties of sea ice. *Cold Regions Science and Technology*, Volume 60, pp. 107-129.

U.S. Department of Commerce, 2007. *Observers' Guide to Sea Ice*, National Environmental Satellite, Data, and Information Service • National Ice Center: National Oceanic and Atmospheric Administration.

Vance, G. P., 1980. *Analysis of the performance of a 140-foot Great Lakes icebreaker: USCGC Katmai Bay*, HANOVER, NEW HAMPSHIRE, U.S.A.: COLD REGIONS RESEARCH AND ENGINEERING LABORATORY.

Wadhams, P., 1986. The Seasonal Ice Zone. In: *The Geophysics of Sea Ice*. s.l.:Springer, Boston, MA, pp. 825-991.

Wan, Z., Ge, J. & Chen, J., 2018. Energy-Saving Potential and an Economic Feasibility Analysis for an Arctic Route between Shanghai and Rotterdam: Case Study from China's Largest Container Sea Freight Operator. *Sustainability*, 10(4).

Weeks, W. F. & Hibler, W. D., 2010. *On Sea Ice*. s.l.:University of Alaska Press.

Woolgar, R. C. & Colbourne, D. B., 2010. Effects of hull-ice friction coefficient on predictions of pack ice forces for moored offshore vessels. *Ocean Engineering*, Volume 37, pp. 293-303.

Appendix A: Results of case study

Table A.1: Broken ice resistance of studied models and model tests in Case 1.

Speed		4.8 knots	5.8 knots	6.8 knots	7.8 knots
Model test [kN]	IMD-493	800	900	1000	1100
	IMD-501	750	800	910	1100
	IMD-614	650	750	900	1100
	IMD-648	1150	1250	1350	1500
	SM-173	2130	2350	2560	2790
The Guo model [kN]	IMD-493	800.98	1011.06	1231.45	1461.49
	IMD-501	800.98	1011.06	1231.45	1461.49
	IMD-614	787.14	993.79	1210.64	1437.03
	IMD-648	807.89	1019.70	1241.86	1473.71
	SM-173	845.93	1067.20	1299.11	1540.95
The Spencer and Jones model [kN]	IMD-493	741.08	795.85	851.23	908.25
	IMD-501	741.08	795.85	851.23	908.25
	IMD-614	728.35	782.52	837.39	893.95
	IMD-648	747.45	802.51	858.15	915.40
	SM-173	782.47	839.15	896.21	954.73

Table A.2: Broken ice resistance of studied models and model tests in Case 2.

Speed		1 knot	3 knots	5 knots
Model tests [kN]	C=60%	114.00	171.02	292.12
	C=80%	384.11	453.50	543.09
	C=90%	414.22	534.74	651.37
The Guo model [kN]	C=60%	28.68	108.00	203.23
	C=80%	56.80	210.05	389.04
	C=90%	75.27	277.07	511.08
The Spencer and Jones model [kN]	C=60%	11.96	20.93	34.48
	C=80%	105.87	143.04	172.45
	C=90%	262.72	346.98	402.88

Table A.3: Brash ice resistance of studied models and model tests in Case 2.

Speed	1 knot	3 knots	5 knots
Model test [kN]	156.95	218.56	339.51
The Spencer and Jones model [kN]	191.70	234.98	292.12
The Riska model [kN]	304.19	333.17	391.62
The Mellor model [kN]	122.55	128.11	139.76

Figure A.4: Brash ice resistance of studied models and model tests in Case 3.

Ice thickness	0.63 m			1.04 m		
	Speed	0.2 m/s	0.5 m/s	1.0 m/s	0.2 m/s	0.5 m/s
Model test [kN]	98	81	69	220	120	210
The Spencer and Jones model [kN]	137.25	140.26	147.03	226.95	232.57	244.67
The Riska model [kN]	271.39	272.91	278.45	477.66	479.94	488.20
The Mellor model [kN]	37.57	37.93	39.29	102.29	102.65	104.01

Appendix B: Results of sensitivity analysis

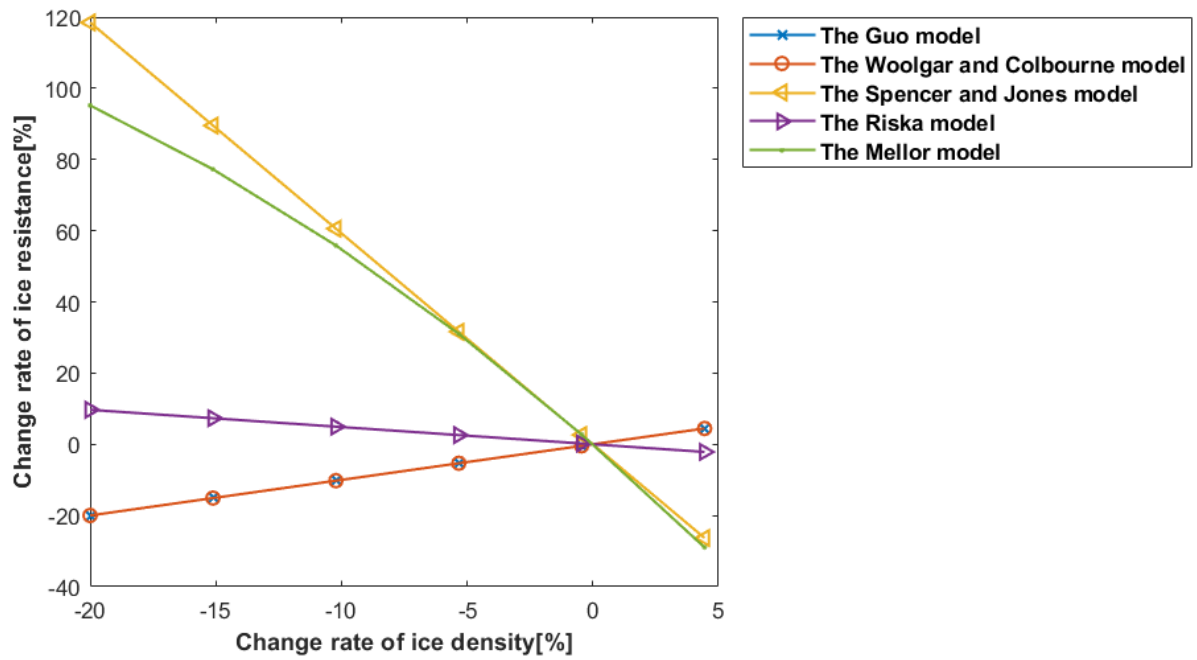


Figure B.1: Sensitivities of ice density. (ship speed = 3 knots).

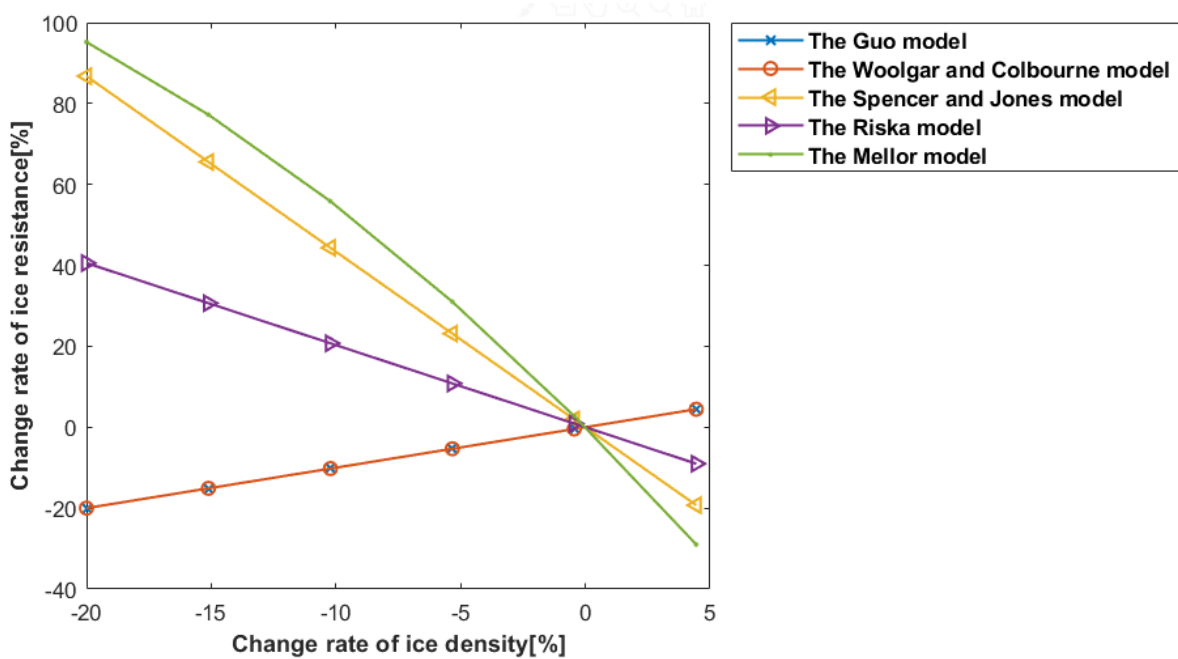


Figure B.2: Sensitivities of ice density. (ship speed = 7 knots).

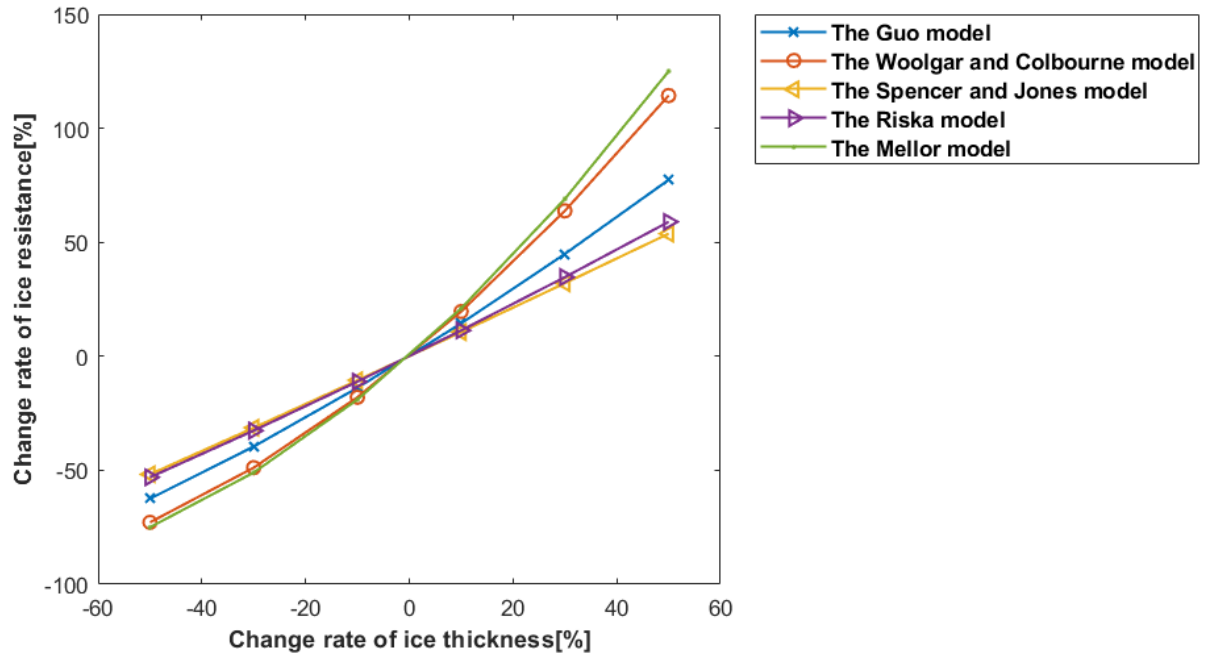


Figure B.3: Sensitivities of ice thickness. (ship speed = 3 knots).

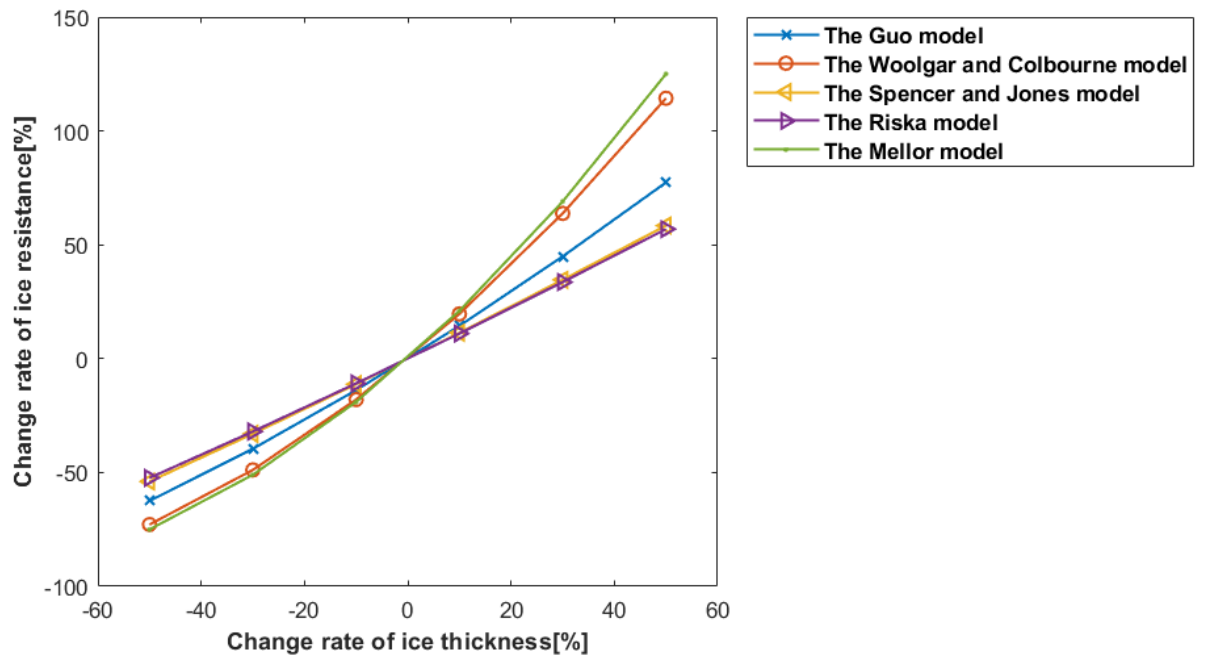


Figure B.4: Sensitivities of ice thickness. (ship speed = 7 knots).

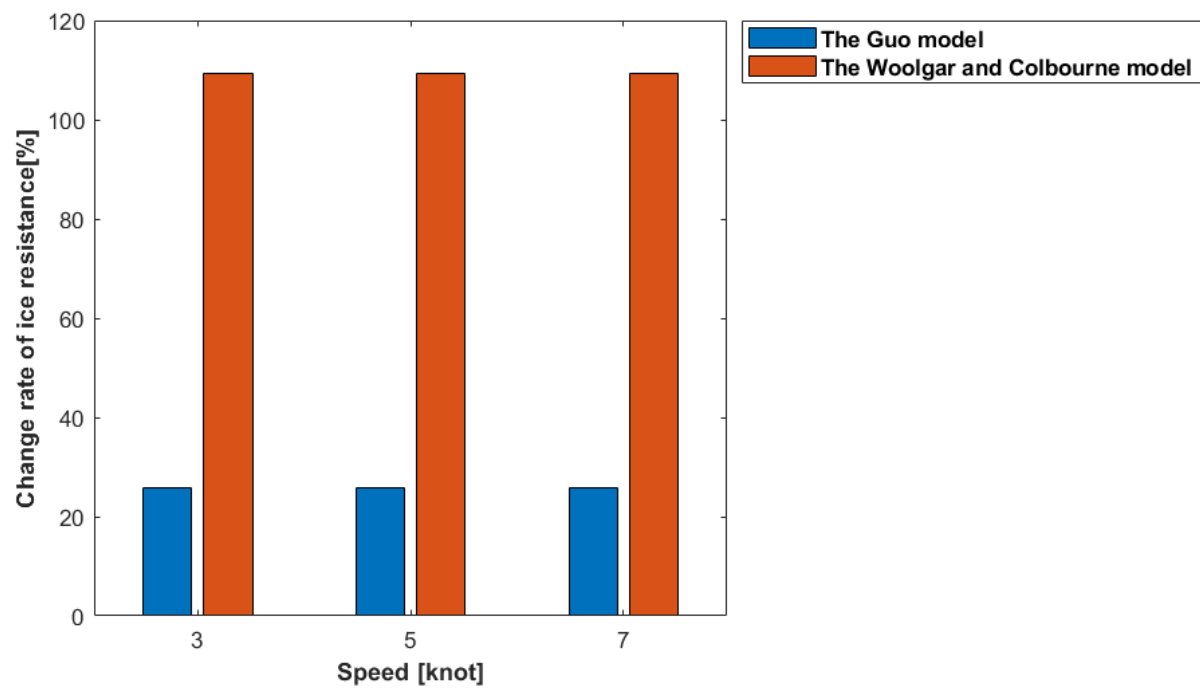


Figure B.5: Sum of sensitivities of ice concentration.

Appendix C: ShipCLEAN results of propulsion power and fuel consumption rate

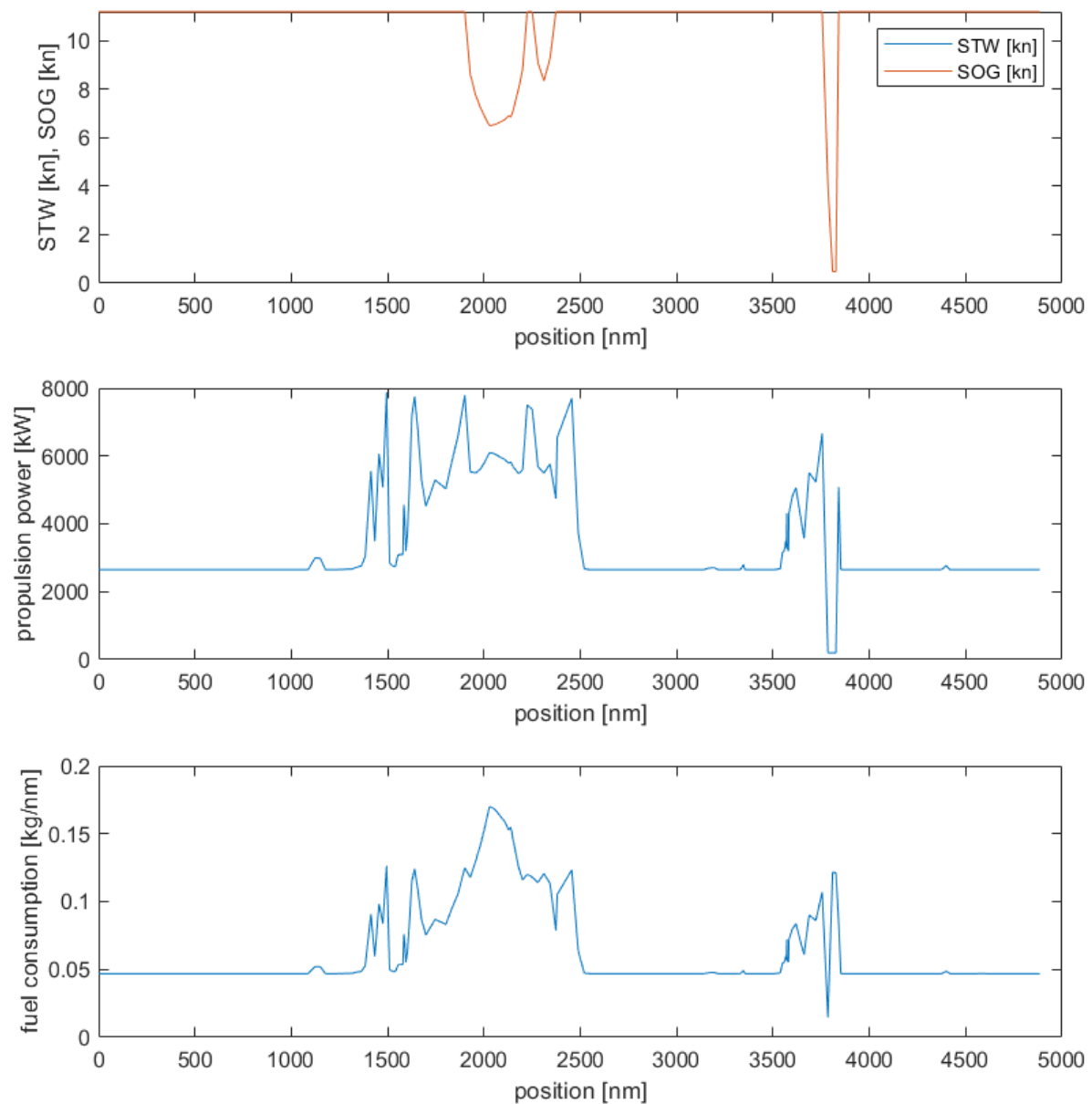


Figure C.1: Ship speed, fuel consumption rate and propulsion power estimations with fixed journey time of 520 hours in 2018 July ice conditions. (The Guo model).

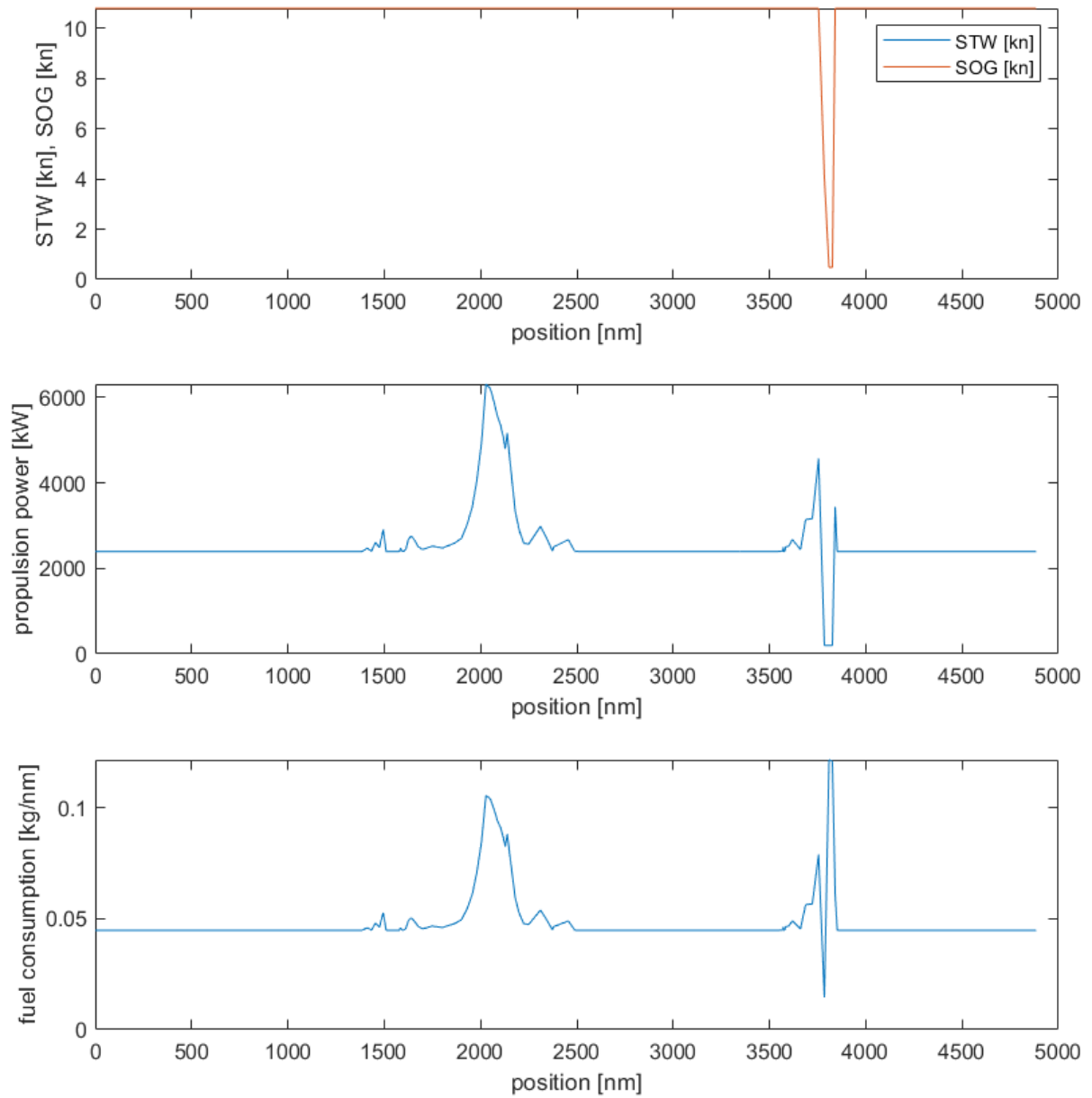


Figure C.2: Ship speed, fuel consumption rate and propulsion power estimations with fixed journey time of 520 hours in 2018 July ice conditions. (The Woolgar and Colbourne model).

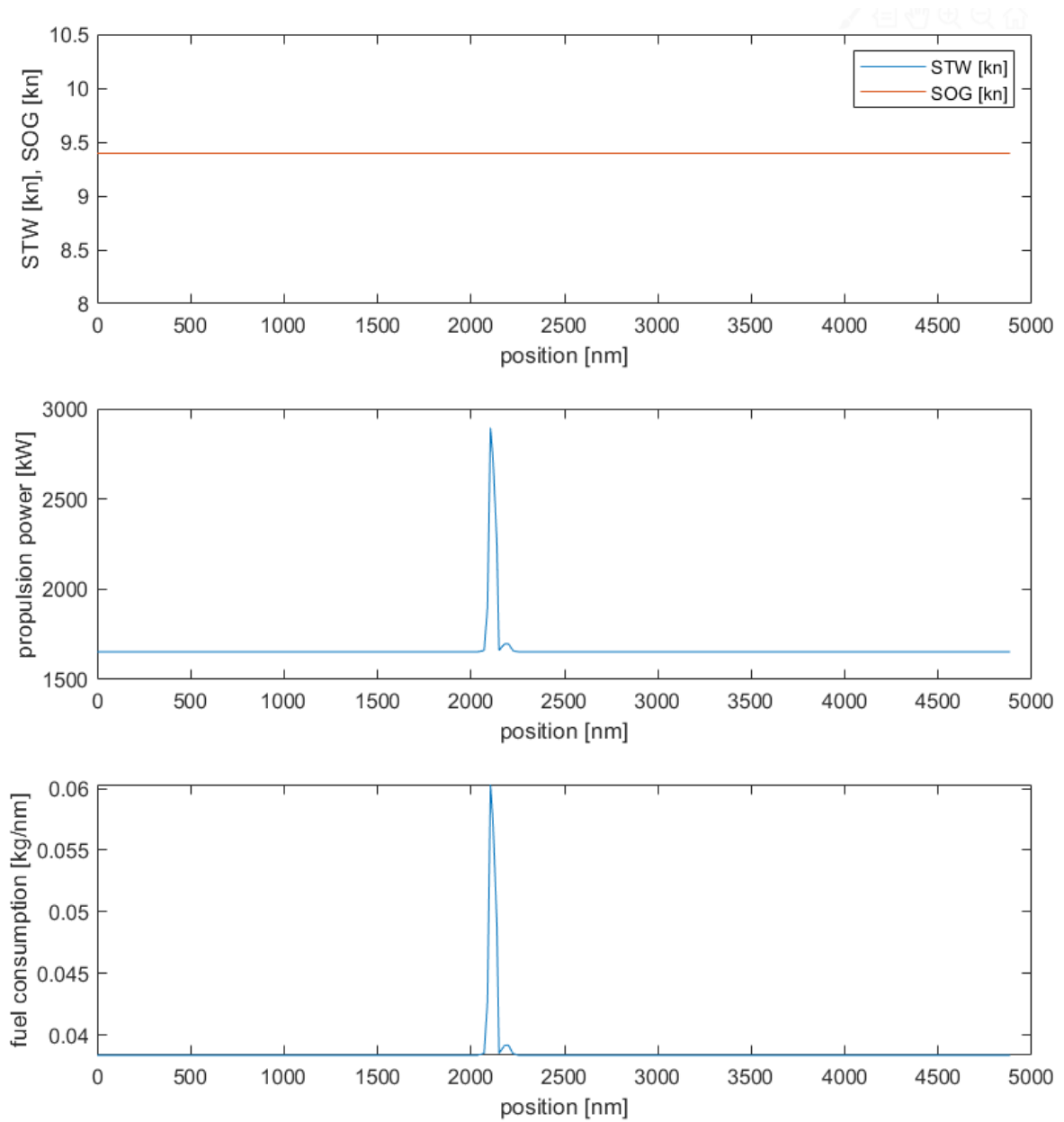


Figure C.3: Ship speed, fuel consumption rate and propulsion power estimations with fixed journey time of 520 hours in 2018 October ice conditions. (The Guo model).

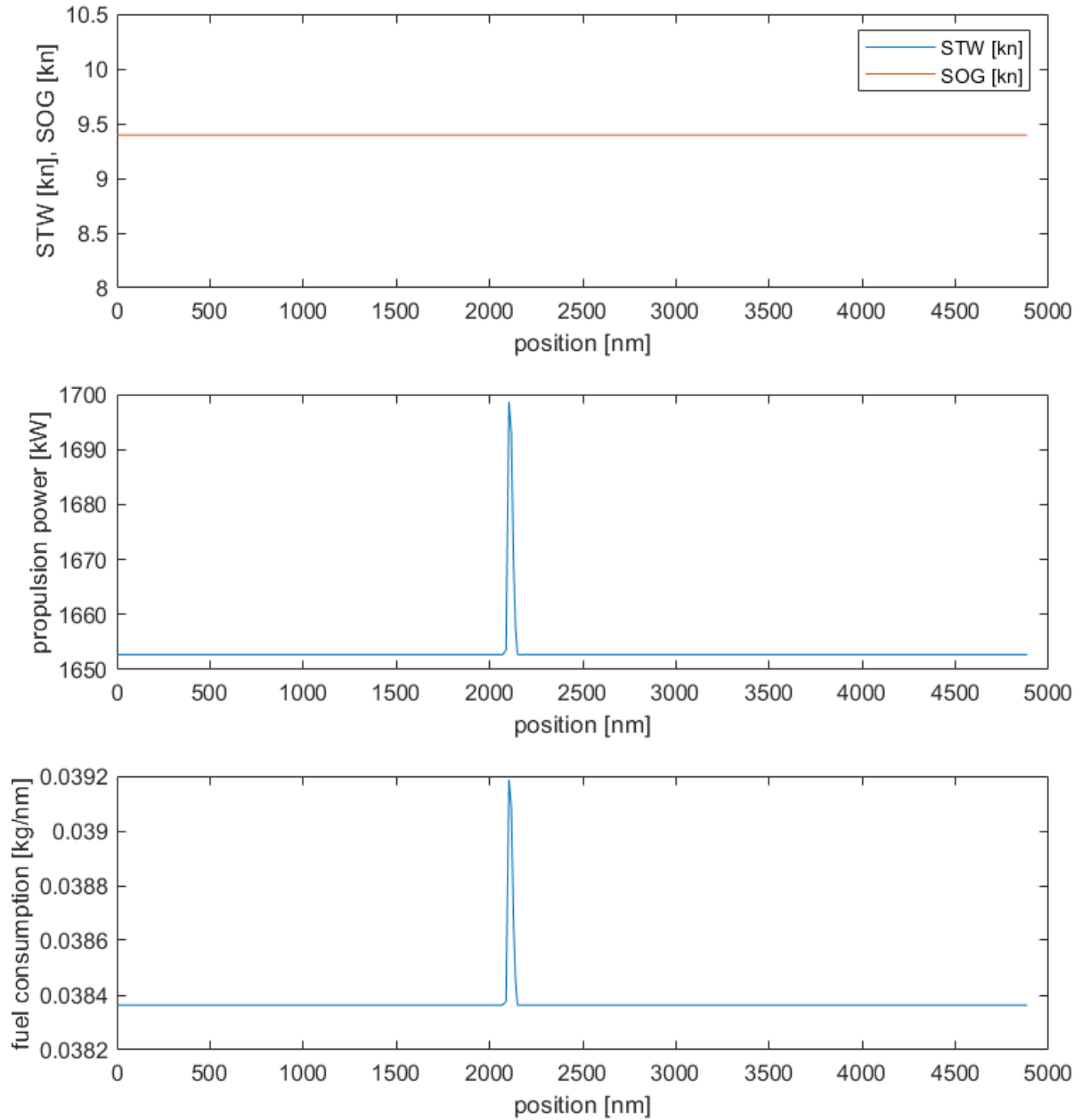


Figure C.4: Ship speed, fuel consumption rate and propulsion power estimations with fixed journey time of 520 hours in 2018 October ice conditions. (The Woolgar and Colbourne model).

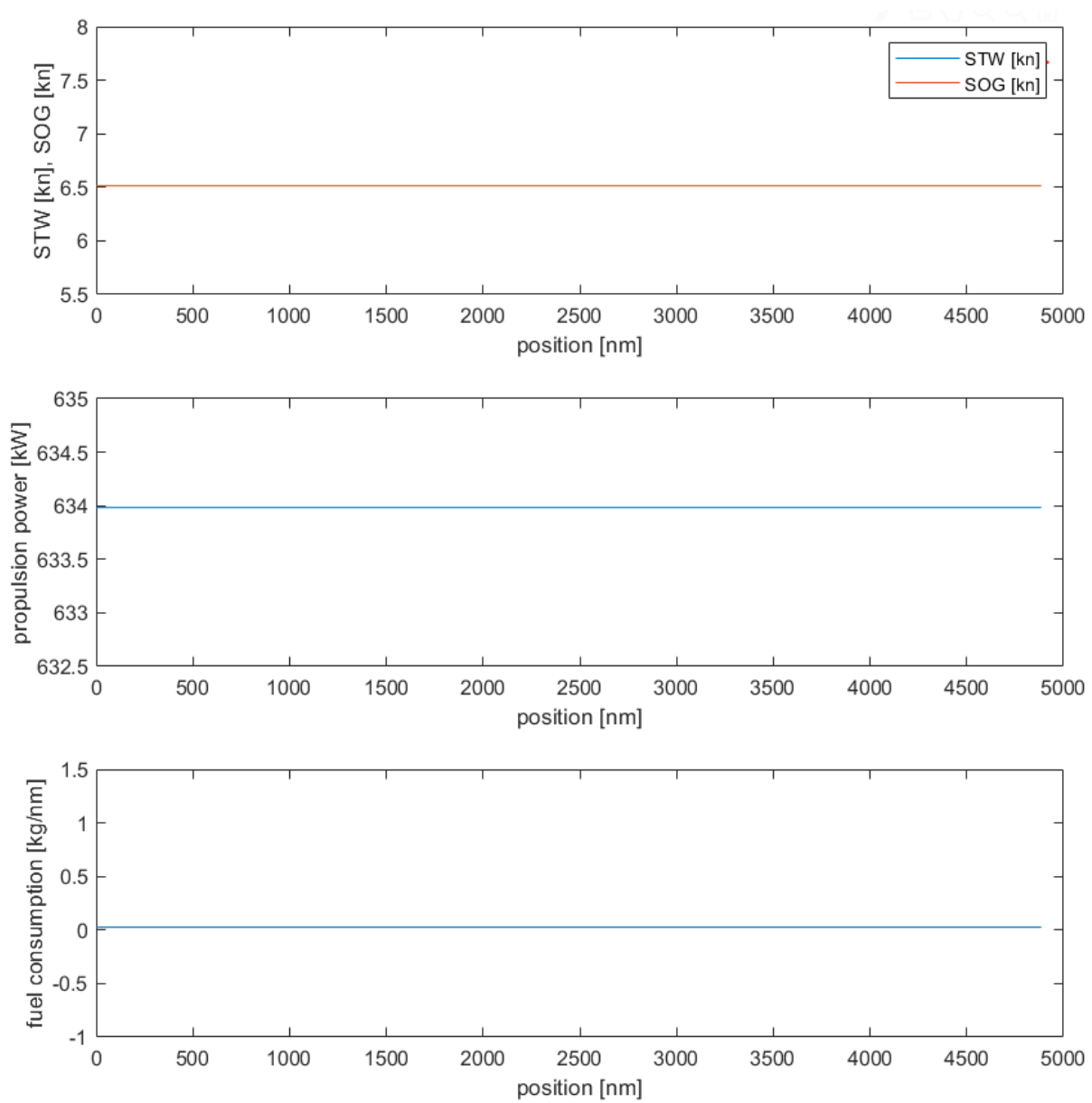


Figure C.5: Ship speed, fuel consumption rate and propulsion power estimations with fixed journey time of 750 hours without ice.

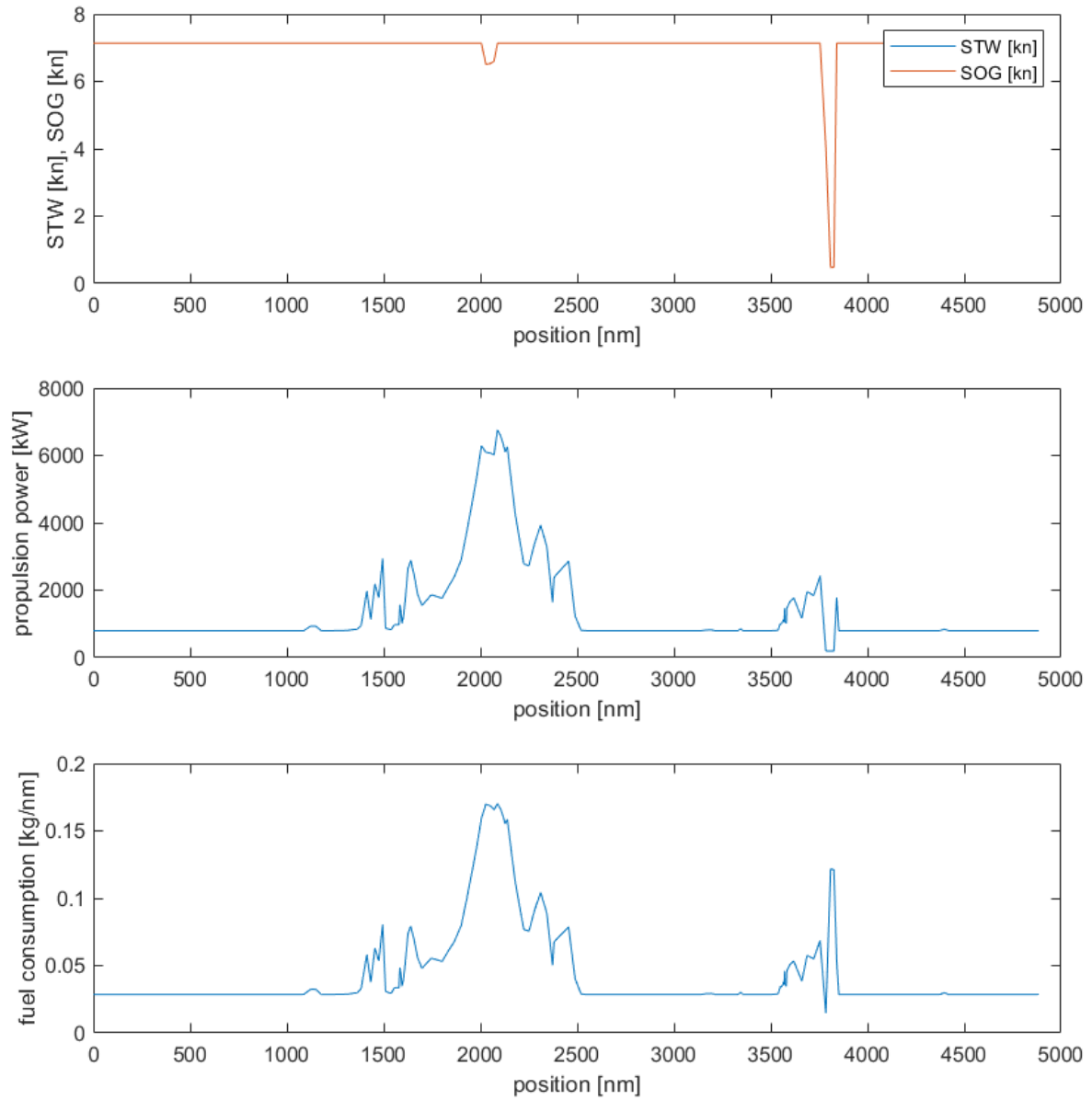


Figure C.6: Ship speed, fuel consumption rate and propulsion power estimations with fixed journey time of 750 hours in 2018 July ice conditions. (The Guo model).

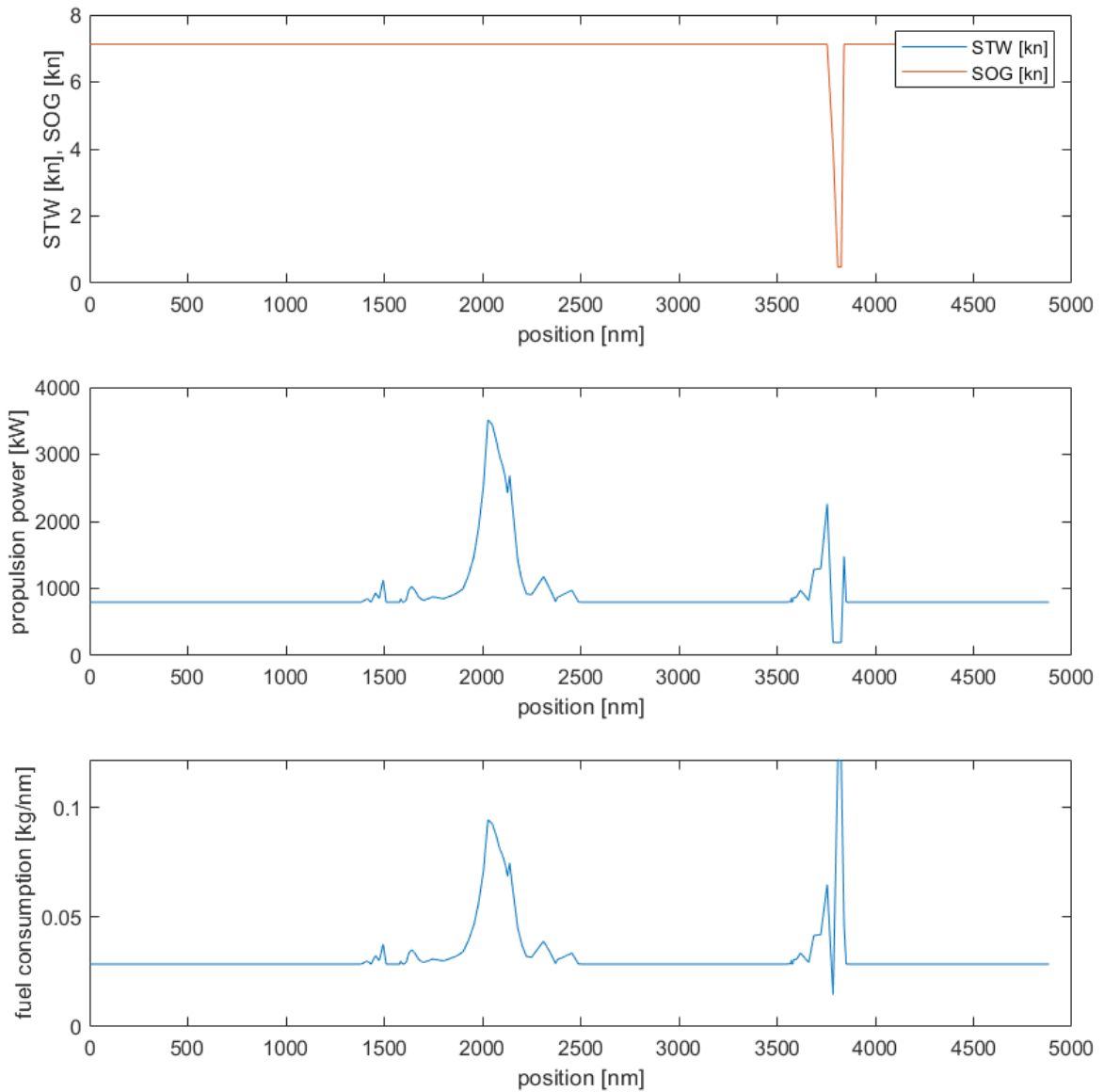


Figure C.7: Ship speed, fuel consumption rate and propulsion power estimations with fixed journey time of 750 hours in 2018 July ice conditions. (The Woolgar and Colbourne model).

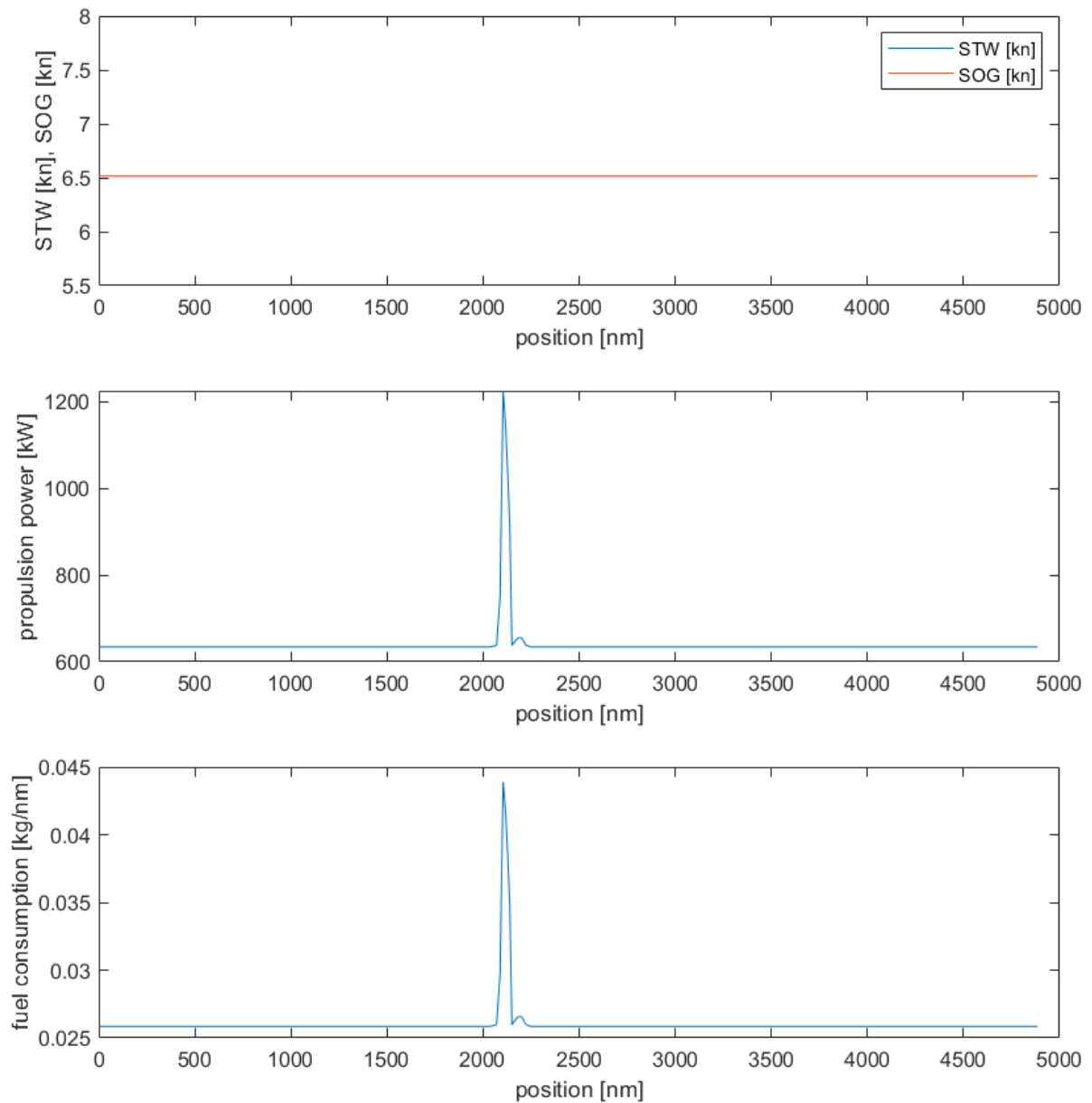


Figure C.8: Ship speed, fuel consumption rate and propulsion power estimations with fixed journey time of 750 hours in 2018 October ice conditions. (The Guo model).

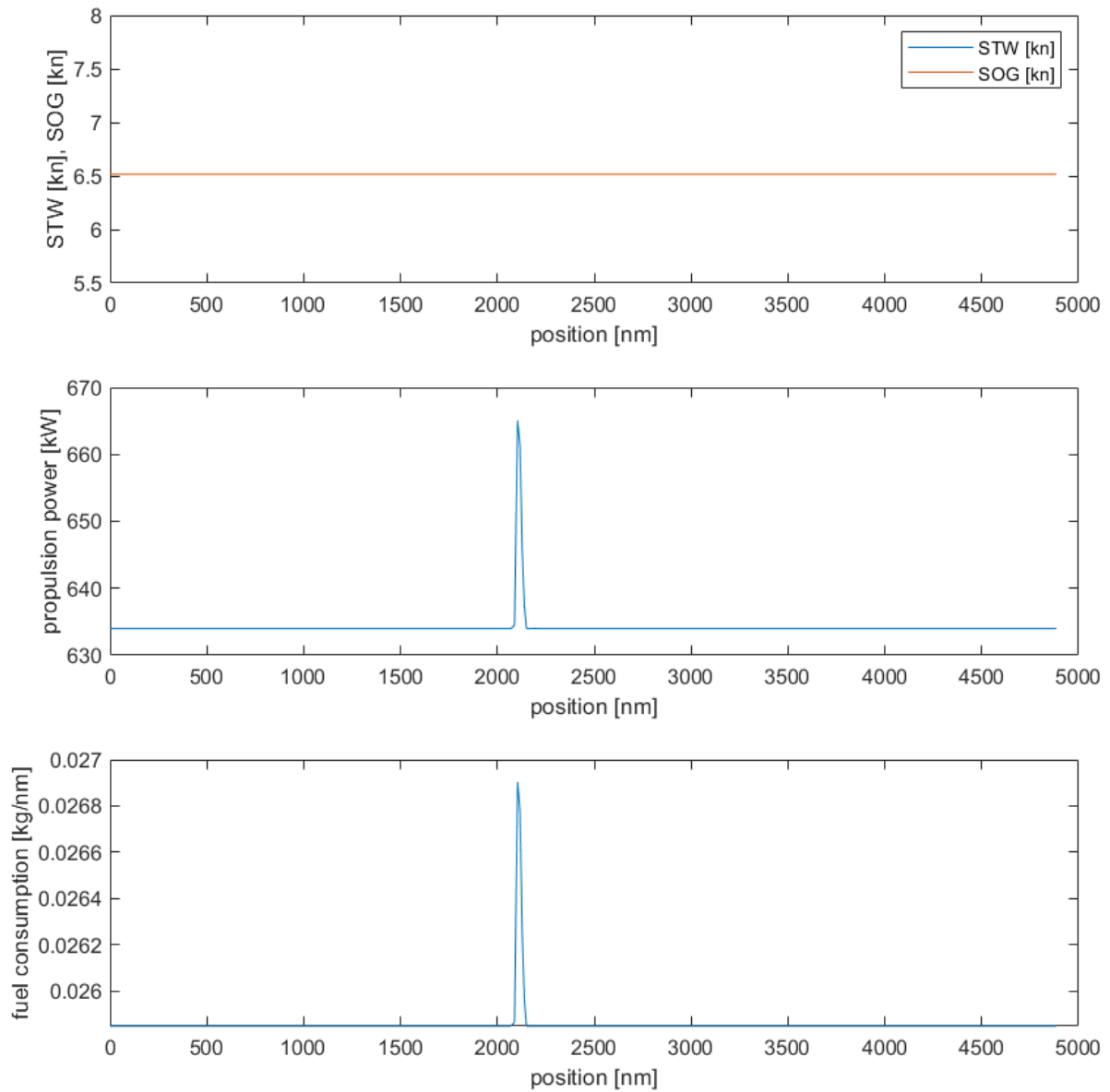


Figure C.9: Ship speed, fuel consumption rate and propulsion power estimations with fixed journey time of 750 hours in 2018 October ice conditions. (The Woolgar and Colbourne model).

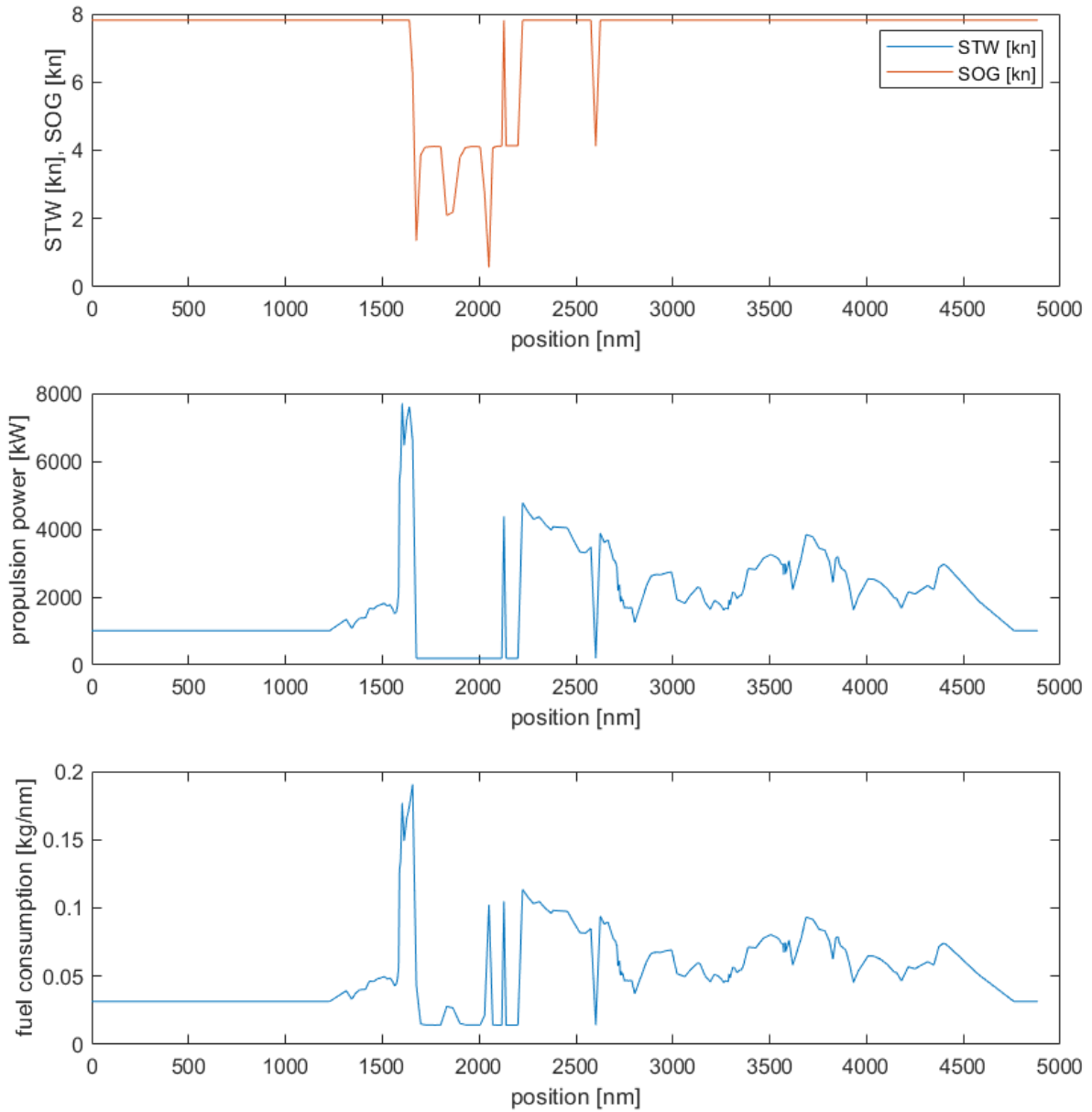


Figure C.10: Ship speed, fuel consumption rate and propulsion power estimations with fixed journey time of 750 hours in 2018 November ice conditions. (The Guo model).

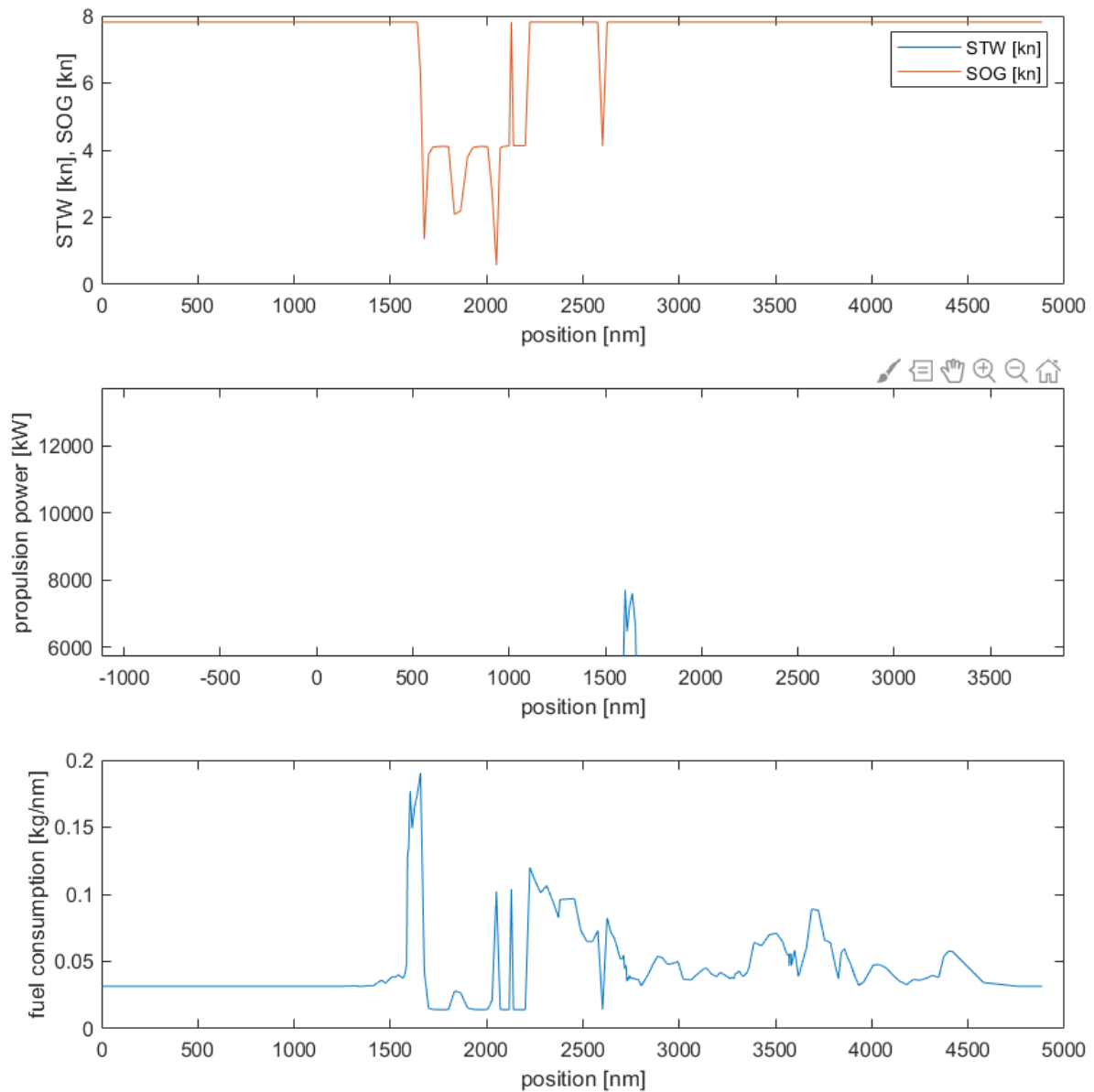


Figure C.11: Ship speed, fuel consumption rate and propulsion power estimations with fixed journey time of 750 hours in 2018 November ice conditions. (The Woolgar and Colbourne model).